



**AUSTRALIAN ATOMIC ENERGY COMMISSION  
RESEARCH ESTABLISHMENT  
LUCAS HEIGHTS**

**FAST FISSION RATIO MEASUREMENTS IN MULTI-ROD CLUSTERS**

by

**A. ROSE  
H.M. JAIN\*  
P.F. MENEZES\***

**\*Bhabha Atomic Research Centre, Trombay, Bombay, India**

**October 1972**

ISBN 0 642 99509 5



AUSTRALIAN ATOMIC ENERGY COMMISSION

RESEARCH ESTABLISHMENT

LUCAS HEIGHTS

FAST FISSION RATIO MEASUREMENTS IN MULTI-ROD CLUSTERS<sup>†</sup>

by

A. ROSE

H.M. JAIN\*

P.F. MENEZES\*

ABSTRACT

A series of Indo-Australian collaborative experiments to measure  $^{238}\text{U}/^{235}\text{U}$  fission rate ratios in  $\text{UO}_2$  rod cluster fuel elements is described. The measurements utilised the well known gross fission product gamma ray counting technique, with calibration by double-fission chamber and  $^{140}\text{La}$  fission product  $\gamma$ -ray counting techniques.

Results are given for fast fission ratios measured over a range of simulated light water coolant densities from zero (air) to one ( $\text{H}_2\text{O}$ ), the mid ranges being covered by high density expanded polystyrene, in clusters of 7, 19, 37 and 61 14.24 mm diameter  $\text{UO}_2$  rods.

---

\* Bhabha Atomic Research Centre, Trombay, Bombay, India.

<sup>†</sup> This work is also reported in IAEC publication, BARC-580.

National Library of Australia card number and ISBN 0 642 99509 5

The following descriptors have been selected from the INIS Thesaurus to describe the subject content of this report for information retrieval purposes. For further details please refer to IAEA-INIS-12 (INIS: Manual for Indexing) and IAEA-INIS-13 (INIS: Thesaurus) published in Vienna by the International Atomic Energy Agency.

CALIBRATION; CONFIGURATION; COOLANTS; COUNTING TECHNIQUES;  
FISSION CHAMBERS; FISSION RATIO; FOILS; FUEL ELEMENT CLUSTERS;  
FUEL RODS; GAMMA DETECTION; GAMMA RADIATION; GEOMETRY;  
IRRADIATION; LANTHANUM 140; LI-DRIFTED GE DETECTORS; POLYSTYRENE;  
SCINTILLATION COUNTERS; SIMULATION; URANIUM DIOXIDE; URANIUM 235;  
URANIUM 238; WATER; ZERLINA REACTOR

## CONTENTS

	<u>Page</u>
1. INTRODUCTION	1
2. FORMAL DESCRIPTION OF METHOD	1
3. THEORY	2
4. EXPERIMENTAL APPARATUS	4
4.1 ZERLINA Reactor	4
4.2 Experimental Clusters	4
4.3 Foils	6
4.4 Counting Apparatus	6
4.5 Double-Fission Chamber	6
5. EXPERIMENTAL METHOD	7
5.1 Cluster Irradiations and Integral Counting Procedure	7
5.2 Calibration Experiments to Determine P(t)	8
6. DETERMINATION OF <sup>235</sup> U CONTENT OF FOIL	11
6.1 Mass Spectrometer Measurements	11
6.2 Thermal Column Measurements	11
6.3 Summary of <sup>235</sup> U Content Measurements for Depleted Uranium Foils	12
6.4 Measurements of Mass Ratio of Electrodeposited Foils	12
7. ERRORS	13
8. $\delta_{28}$ RESULTS	15
9. SUMMARY AND CONCLUSION	15
10. ACKNOWLEDGEMENTS	16
11. REFERENCES	17
TABLE 1 Multi-rod Clusters and Cluster Coolants Used in Fast Fission Measurements	
TABLE 2 Comparison of P(t) Values	
TABLE 3 Mass Spectrometer Measurements	
TABLE 4 Depleted Uranium Foil Enrichment	
TABLE 5 Errors in the Measurement of $\delta_{28}$	
TABLE 6a Fast Fission Ratios in Clusters Ge(Li) Results	

CONTENTS (Cont'd.)

Page

TABLE 6b	Fast Fission Ratios in Clusters (NaI Results)	
TABLE 6c	Fast Fission Ratios in Clusters (Mean of NaI and Ge(Li) Results)	
FIGURE 1	Vertical cross section of ZERLINA	
FIGURE 2	Cross section of ZERLINA core	
FIGURE 3	Cluster details	
FIGURE 4	Photograph of demountable rod	
FIGURE 5	Details of fuel rods and assembly of 7-rod cluster	
FIGURE 6	Details of housing tubes	
FIGURE 7	Cross section of mouldings	
FIGURE 8	7 and 19-rod clusters	
FIGURE 9	37-rod cluster with housing tube	
FIGURE 10	Section of 19-rod cluster showing foil packet	
FIGURE 11	Complete 37-rod cluster	
FIGURE 12	Diagrams of electronics used in counting systems	
FIGURE 13	Double fission chamber	
FIGURE 14	Decay of $^{140}\text{La}$	
FIGURE 15	Gamma ray spectra from uranium fission products	
FIGURE 16	Foil locations in thermal column	
FIGURE 17	Comparison of depleted foil enrichment	
FIGURE 18	Schematic diagram showing steps in determination of $\delta_{28}$	
FIGURE 19	Variation of $\delta_{28}$ with hydrogen atoms in coolant for various cluster geometries	
FIGURE 20	Comparison of gamma decay from natural and depleted uranium	

## 1. INTRODUCTION

In boiling light water cooled heavy water moderated power reactors, the low boiling point of light water necessitates that fuel and coolant operate at high pressure in a suitable pressure tube array if reasonable thermodynamic efficiency is to be achieved. The coolant density can then vary significantly along the fuelled region, and with changing operating conditions. A good knowledge and understanding of the effects of coolant density changes on the physics of the reactor is therefore essential if safety and control requirements of the system are to be reliably assessed.

One important parameter significantly sensitive to coolant density is the contribution of fast fissions in  $^{238}\text{U}$  to system reactivity, and it is important to design surveys that the variation of this parameter with coolant density, cluster geometry, etc. is predicted adequately. The adequacy of calculational methods to predict these changes is usually assessed by comparison with the experimentally measurable parameter  $\delta_{28}$  which is defined as the ratio of  $^{238}\text{U}$  to  $^{235}\text{U}$  fission rates in the fuel element.

Valid simulation of light water coolant densities typical of operating power reactors has always presented problems under the conditions of zero energy reactor physics experiments. In addition,  $\delta_{28}$  measurements are subject to systematic errors and experiments using a common technique covering a wide range of cluster geometry and coolant density combinations would make a valuable addition to the existing experimental data.

These requirements are met by the present measurements which were made as a collaborative project between the Australian and Indian Atomic Energy Commissions in the Bhabha Atomic Research Centre (BARC) zero energy reactor ZERLINA, at Trombay, India. Fast fission ratios,  $\delta_{28}$  were measured for fuel clusters containing 7, 19 37 and 61 14.24 mm diameter  $\text{UO}_2$  rods, with constant spacing. The measurements were also made in 7 and 19 clusters with a much increased rod spacing. In all geometries the variation of  $\delta_{28}$  was investigated as the inter-rod coolant density was varied. 'Coolants' of air and full density room temperature  $\text{H}_2\text{O}$  were used in all geometries, and further measurements with intermediate simulated  $\text{H}_2\text{O}$  densities of  $0.25 \text{ g/cm}^3$  and  $0.64 \text{ g/cm}^3$  were made in a representative range of geometries by using high density expanded polystyrene mouldings.

## 2. FORMAL DESCRIPTION OF METHOD

The method used is based on a comparison of the gross fission product gamma activities of natural and depleted uranium foils irradiated in selected fuel rods in the clusters. The measured gamma activity ratio is related to the

true fission ratio by a calibration factor  $P(t)$  which was determined using the technique of Wolberg et al. (1964), and also by double-fission chamber measurements.

The technique of Wolberg et al. measures the relative activity of the 1.60 MeV gamma ray of the fission product  $^{140}\text{La}$  for a depleted and natural uranium foil, and relates these to the actual foil fission rates via the published yields of  $^{140}\text{La}$  in  $^{238}\text{U}$  and  $^{235}\text{U}$  fission. Since a high resolution lithium drifted germanium detector was available for the experiments, an attempt was made to locate some lower energy fission product gamma ray with more convenient counting properties than  $^{140}\text{La}$ , but nothing suitable was detected.

The double-fission chamber method measures the ratio of fission from thin films of natural and depleted uranium, and relates this ratio to the fission product gamma activity ratio of thicker natural uranium and depleted uranium foils irradiated simultaneously inside the same chamber. From these ratios the calibration factor  $P(t)$  is determined directly.

The gross fission product gamma activities were measured on both the germanium detector counting system and a sodium iodide crystal, thus providing two sets of data. As the calibration factor  $P(t)$  is not the same for both counting systems it was determined separately for each.

### 3. THEORY

The  $^{238}\text{U}$  to  $^{235}\text{U}$  fission rate ratio,  $\delta_{28}$ , in fuel clusters can be written as

$$\delta_{28} = \frac{N^{28} \int_0^{\infty} \sigma_f^{28}(E) \phi(E) dE}{N^{25} \int_0^{\infty} \sigma_f^{25}(E) \phi(E) dE} \quad \dots (1)$$

where superscripts 28 and 25 denote  $^{238}\text{U}$  and  $^{235}\text{U}$  respectively

$N$  is the atomic density,

$\sigma_f(E)$  the fission cross section

and  $\phi(E)$  the energy dependent neutron flux.

In practice, fissionable detector foils contain a mixture of  $^{238}\text{U}$  and  $^{235}\text{U}$  isotopes; therefore  $\delta_{28}$  cannot be measured directly. Rather it must be inferred from the relative fission product gamma activities of two foils of differing enrichments via a separate calibration experiment.

If thin foils of natural and depleted uranium are irradiated at the same

position in a fuel cluster and the resulting fission product activities counted in some specified way, we may define the ratio

$$\gamma(t) = \frac{\text{measured fission product decay activity from depleted foil}}{\text{measured fission product decay activity from natural foil}}$$

Using the notation of Wolberg et al.  $\delta_{28}$  for a natural uranium fuel cluster is then related to  $\gamma(t)$  through the expression

$$\delta_{28} = P(t) (a\gamma(t) - s) / (1 - a\gamma(t)) \quad \dots(2)$$

where

$$a = \frac{1+R_1}{1+R_2}, \quad s = \frac{R_1}{R_2}$$

and

$$R_1 = \frac{\text{number of atoms of } ^{235}\text{U in depleted foil}}{\text{number of atoms of } ^{238}\text{U in depleted foil}}$$

and

$$R_2 = \frac{\text{number of atoms of } ^{235}\text{U in natural foil}}{\text{number of atoms of } ^{238}\text{U in natural foil}}$$

$P(t)$  is a time dependent calibration factor which depends on the fission product yields, the counter characteristics, the length of the foil irradiation and the time and duration of the gamma-counting.

In the method of Wolberg et al. for the determination of  $P(t)$ , a pair of uranium foils, one depleted and one natural, is irradiated simultaneously in a reference position. After allowing time for decay of  $^{140}\text{Ba}$  and build-up of  $^{140}\text{La}$ , the ratio  $\gamma$ , the number of  $^{140}\text{La}$  1.6 MeV gamma counts from the depleted foil to that from the natural foil, is measured.  $\gamma$  is then related to  $\delta_{28}$  by

$$\delta_{28} = (\beta_{25}/\beta_{28}) [a\gamma - s] / [1 - a\gamma] \quad \dots(3)$$

where the betas are the fission product yields of  $^{140}\text{La}$  from  $^{238}\text{U}$  and  $^{235}\text{U}$  fission.

Once  $\delta_{28}$  has been determined for the reference position, a pair of foils similar to those used in the cluster fuel elements is irradiated in the reference position for the standard time and  $\gamma(t)$  found in the usual manner. From Equation (2)  $P(t)$  can then be found.

In the alternative double-fission chamber technique to determine  $P(t)$ , depleted and natural electroplated foils are used as the fissile coatings in a two-chamber counter. Standard type depleted and natural foils are also included at the centre of the counter, which is irradiated for the standard

time, during which the relative count rates from the electrodeposited foils are measured. At the end of the irradiation, the standard foils are removed from the counter and gamma counted by the standard technique to give  $\gamma'(t)$ , similar to  $\gamma(t)$  from the cluster irradiations. From the fission chamber counting  $F$  is obtained where

$$F = \frac{\text{fissions from electrodeposited depleted foil in counter}}{\text{fissions from electrodeposited natural foil in counter}}$$

whence  $P(t)$  is given by the relation

$$P(t) = \left[ \frac{1 - a\gamma'(t)}{a\gamma'(t) - s} \right] \left[ \frac{aMF - s}{1 - aMF} \right] \quad \dots(4)$$

where  $a$  and  $s$  are as before and  $M$  is a factor to account for mass and thickness differences between the electrodeposited foils.  $M$  is determined by irradiation of the double-fission chamber containing the electrodeposited foils in a well thermalised flux, and measuring the  $^{235}\text{U}$  fission rate for each foil.

#### 4. EXPERIMENTAL APPARATUS

##### 4.1 ZERLINA Reactor

ZERLINA is a heavy water moderated zero energy reactor which is well suited to lattice experiments. Probhakar et al. (1962) have given a detailed description of the reactor, so only the points affecting the present measurements will be given here.

The reactor (Figure 1) consists of a cylindrical aluminium tank having an inner diameter of 2286 mm and a height of 4350 mm. A radial graphite reflector 735 mm thick and 3000 mm high surrounds the tank. The bottom graphite reflector is 815 mm thick. Reactivity is controlled by raising or lowering the  $\text{D}_2\text{O}$  level and the maximum  $\text{D}_2\text{O}$  level allowed for these experiments was 1960 mm.

The core, normally consisting of 80 natural uranium metal rods, 2438 mm long and 35.6 mm diameter forming a lattice with a square pitch of side 190 mm, had the nine central rods removed for the present experiments. This made available a  $\text{D}_2\text{O}$  region of approximately 600 mm diameter. For each  $\delta_{28}$  measurement, a single rod cluster in its housing tube was located on the axis of this central  $\text{D}_2\text{O}$  region. The influence of the uranium metal fuel rods on the  $\delta_{28}$  measurements was therefore kept small. A diagram of the lattice arrangement is given in Figure 2.

##### 4.2 Experimental Clusters

Clusters of 7, 19, 37 and 61 rods with rod centre to centre spacing of

~ 17 mm were studied. In addition the 7 and 19-rod clusters were used with spacing of ~ 24 mm. Details of the clusters are shown in Figure 3. Water, air, and expanded polystyrene foam at two densities were used in different experiments to represent 'the coolant' filling the housing tubes (see Table 1).

#### 4.2.1 Cluster fuel rods

Clusters were assembled from UO<sub>2</sub> fuel rods each made up of approximately 67 UO<sub>2</sub> pellets, 14.24 mm diameter and density 10.3 g/cm<sup>3</sup>, sealed in an aluminium tube. The tube thickness was 0.73 mm and radial clearance between pellets and tube was 0.07 mm. The fuelled length was 1200 mm. Special demountable rods were fabricated so that the foil packet, consisting of 0.05 mm aluminium guard foil, depleted uranium foil, aluminium guard foil, natural uranium foil and aluminium guard foil, could be placed between fuel pellets midway along the rod. Four precision surface ground pellets were kept on either side of the foil packet with seven selected quality standard finish pellets on either side of these. This ensured that the foil environment was for all practical purposes a solid rod of UO<sub>2</sub>. The remaining tube space was filled with lower grade pellets of lengths such that the foil packet was located exactly 572.7 mm from the inside surface of the bottom sealing plug. The several demountable rods used were carefully machined and selected to be as similar as possible. Figure 4 shows a demountable rod with foil packets in position.

#### 4.2.2 Cluster end plates and spacer plates

The cluster spacing was set by the end plates, but spacer plates, machined to the same accuracy as the end plates, placed at intermediate positions along the clusters were found necessary to overcome the effects of 'bowing'. An exploded view of a complete cluster is given in Figure 5.

#### 4.2.3 Cluster housing tubes

The clusters were housed in aluminium tubes, the details of which are given in Figure 6. The wide spaced 7-rod cluster was housed in the standard spaced 19-rod cluster housing tube and the wide spaced 19-rod cluster was housed in the standard spaced 37-rod cluster housing tube.

#### 4.2.4 Polystyrene 'coolant'

To simulate two-phase water/steam coolant at densities appropriate to operating power reactors, expanded polystyrene (C<sub>8</sub>H<sub>8</sub>)<sub>n</sub> was used at densities of 0.64 g/cm<sup>3</sup> and 0.25 g/cm<sup>3</sup>. At these densities the hydrogen atom concentrations are 2.965 x 10<sup>22</sup> and 1.158 x 10<sup>22</sup> cm<sup>-3</sup> respectively. Moulding was successfully carried out to very close tolerances (±0.04 mm) using techniques described by Rose (1970). Mouldings each 152.4 mm long were made for 7, 19 and 37-rod standard spaced clusters and for the wide spaced 19-rod cluster.

Seven mouldings were used for each cluster geometry (see Figures 7 and 8).

#### 4.2.5 Cluster assembly

The clusters were assembled using the components shown in Figure 5, and then connected to an extension rod before sealing into the housing tube. For water 'cooled' clusters the water level in the tube was set and monitored using a transistorised level indicator (Mistry 1968). Details and photographs of a complete cluster assembly are shown in Figures 9, 10 and 11.

### 4.3 Foils

#### 4.3.1 Foils for integral counting

Natural and depleted uranium foils with thicknesses ranging from 0.10 to 0.15 mm were machined to the diameter of the fuel pellets (14.24 mm). Foil diameters were kept within the range  $14.24 \pm 0.02$  mm. The foils were degreased in acetone and the oxide film removed by dissolving in dilute nitric acid. After washing and drying the foils were weighed. The foils had a bright metallic appearance at this stage, but soon turned brown as the oxide layer reformed. However oxide reformation was slow and over a period of two months check weighings showed that the increase in foil mass due to oxide layers was less than 0.01 per cent.

#### 4.3.2 Fission chamber electroplated foils

The uranium fission foils were made by electrolytic deposition of natural uranium and depleted uranium respectively, onto stainless steel discs. The discs were 25.4 mm diameter and 0.127 mm thick with the uranium deposit covering  $366 \text{ mm}^2$ . Details of the determination of the relative concentration of  $^{235}\text{U}$  in the deposited foils are discussed in section 6.4.

### 4.4 Counting Apparatus

For foil counting, two independent systems were used. These consisted of a NaI crystal with associated electronics and a lithium drifted germanium crystal with associated electronics; block diagrams of electronics used for both systems are shown in Figures 12a and 12b.

#### 4.5 Double-Fission Chamber

The double-fission chamber was of the gas flow type and used 90 per cent argon, 10 per cent methane as the counting gas. It consisted of two chambers made from 2S aluminium and is shown in Figure 13.

The uranium fission foils fit inside the counter, a gap being left between them to accommodate two standard uranium foils and aluminium spacers (see Figure 13).

Output pulses from each chamber were recorded simultaneously on two counting channels.

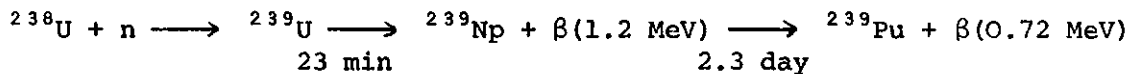
## 5. EXPERIMENTAL METHOD

### 5.1 Cluster Irradiations and Integral Counting Procedure

It was usual to irradiate three sets of foils, each set consisting of a depleted uranium and a natural uranium foil. Prior to irradiation, the background activities of the foils were determined and the foil then loaded into the demountable rods (see Figure 4) which were then inserted into the cluster. The position of these rods in the cluster had been chosen when the cluster end plates were being manufactured and were as shown in Figure 3. As can be seen from this figure, rod symmetry requires that only two measuring positions will satisfy the 7-rod cluster, three the 19-rod cluster, five the 37-rod cluster and eight the 61-rod cluster. Allowance was made in the cluster end plates to accommodate more than this minimum, but as time was limited only the positions shown in Figure 3 were used.

With the foils loaded and the cluster in the housing tube with the desired coolant, the complete assembly (see Figure 10) was loaded into the reactor and irradiated for two hours at 100 watts ( $\sim 1 \times 10^8$  n/cm<sup>2</sup>/sec). This two hour irradiation and 100 watt power level was used for all cluster irradiations except the BARC <sup>140</sup>La calibration where irradiation was for 20 hours at 100 watts.

After shutdown it was necessary to allow the cluster to 'cool' for two hours before removal from the reactor. The foils were then removed ready for counting. If we consider the <sup>238</sup>U neutron capture reaction and the decay chain of the resulting <sup>239</sup>U nuclide



it is clear that care must be taken to ensure that bremsstrahlung originating from the decay betas is not counted. For the integral counting, both NaI and Ge(Li) systems used a discriminator setting equivalent to 0.75 MeV and foil counting was started 3 hours after reactor shutdown. The 0.75 MeV setting ensured that bremsstrahlung from the beta activity of the <sup>239</sup>Np ( $E_{\text{max}}^{\beta-} = 0.72 \text{ MeV}$ ) was not counted and the 3 hour 'cooling' period ensured that there was negligible contribution from <sup>239</sup>U ( $E_{\text{max}}^{\beta-} = 1.2 \text{ MeV}$ ) which has a 23 minute half life (Wolberg et al. 1964).

Foil sets were counted in rotation on both NaI and Ge(Li) systems, and the foils themselves were counted in turn starting with the depleted uranium, then the natural uranium then the depleted uranium, and this sequence repeated until sufficient counts had been obtained. The counting period was two minutes for

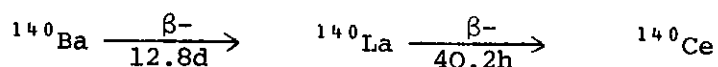
the depleted uranium foils and one minute for the natural uranium foils. The counting efficiency of the NaI system was about five times that of the Ge(Li) system.

## 5.2 Calibration Experiments to Determine P(t)

### 5.2.1 $^{140}\text{La}$ measurements on NaI crystal

The counting system differed from that shown in Figure 12a in that the output from the NaI system's amplifier was fed directly into the 512 channel analyser.

A standard natural uranium foil and a standard depleted uranium foil of similar mass were irradiated in the R<sub>1</sub> position (see Figure 3) of the 37-rod (air 'coolant') cluster for 20 hours at 100 watts. Irradiations at higher power levels and longer times were not permitted by the Reactor Operation Standing Orders. After irradiation, the foils were removed from the cluster and allowed to 'cool' for a minimum of 16 days to allow the 40 hour half life activity in the chain



to reach equilibrium with its parent 12.8 day  $^{140}\text{Ba}$ , before counting of the 1.6 MeV gamma ray associated with  $^{140}\text{La}$  was started. The amplifier gain was set so that the 1.6 MeV gamma ray peak position was centred on a particular channel of the analyser and all further counting of this type followed the same setting-up procedure. Counting was carried out at regular intervals over a period of about two weeks, and on completion the output from the analyser store, covering the peak region was printed out. It should be noted that, whilst the Ge(Li) counting channel was extremely stable, problems with amplifier gain stability in the NaI counting channel restricted counting times with that equipment to 40 minutes only without resetting.

### 5.2.2 $^{140}\text{La}$ measurements on Ge(Li) detector

Because of the lower efficiency of the Ge(Li) detector, the  $^{140}\text{La}$  activity on the uranium foils after the 2000 watt hours irradiation was insufficient to give adequate counting statistics. Calibration of the Ge(Li) detector system was therefore done after its return to Australia, using the reactor MOATA (Marks 1962) for the necessary foil irradiations.

The pneumatic facility on MOATA provided a reproducible position close to the core, and the double-fission chamber (see Figure 13) was located at this position. A standard natural uranium foil and a standard depleted uranium foil, separated by 0.00076 mm Al, were located at the centre of the double-fission chamber and irradiated for 14 hours at 6 kilowatt ( $\sim 6 \times 10^{10}$  n/cm<sup>2</sup>/sec).

After irradiation, the foils were allowed to 'cool' as described in Section 5.2.1 before counting the 1.6 MeV gamma ray. The Ge(Li) counting system was unchanged except that the output from the bias amplifier was fed directly into the multichannel analyser, the amplifier gain having been adjusted to locate the 1.6 MeV gamma peak in a central channel. Foil counting times up to 800 minutes were used, and counting which commenced 16 days after the irradiation was done at intervals of a few days over a period of six weeks. After 16 days the  $^{140}\text{La}$  was in equilibrium with the parent  $^{140}\text{Ba}$  and, as can be seen from Figure 14, decaying with a 12.8 day half life. The stability of the Ge(Li) system electronics was excellent and no drift was observed in the 1.6 MeV gamma ray peak position over the counting time used.

### 5.2.3 Analysis of $^{140}\text{La}$ data

The output from the  $^{140}\text{La}$  counting from both NaI and Ge(Li) systems was obtained from the analyser print out. Typical outputs (Figure 15) show that the  $^{140}\text{La}$  gamma ray of 1.6 MeV dominates the gamma spectrum for both the natural uranium and the depleted uranium foils. The energy resolution is, of course, superior in the case of the Ge(Li) system. From these analyser outputs a determination was made of the total counts under the respective 1.6 MeV gamma peaks. A first or second degree polynomial fit was made to a number of channels on either side of the peak and the background at each channel under the peak determined. Background was subtracted channel for channel and the integral peak count obtained. The analysis was done using the computer program PTVAl (Rose 1969), and the results used to form the ratio of depleted  $^{140}\text{La}$  counts to natural  $^{140}\text{La}$  counts. This ratio was corrected for foil mass etc. to yield the value of  $\gamma$  for use in equation (3). Then, using the value of  $1.055 \pm 0.03$  (Ciuffolotti 1969) for  $\beta_{25}/\beta_{28}$  and the values calculated for  $a$  and  $S$ , the parameter  $\delta_{28}$  was determined for the measuring position. As  $\gamma(t)$  for the NaI calibration position (R1 in 37-rod air cluster) and  $\gamma'(t)$  for the Ge(Li) calibration position (pneumatic facility of MOATA) had been measured, the respective value of  $P(t)$  was deduced for each counting system from Equation (2). The values obtained for  $P(t)$  by the above techniques are listed in Table 2.

### 5.2.4 Double-fission chamber measurements

These measurements were also carried out in MOATA, using the Ge(Li) counting system only. The measuring position was the 'fully in' position of the MOATA pneumatic facility, identical to that used for the Ge(Li)  $^{140}\text{La}$  measurements. A standard natural uranium foil and a standard depleted uranium foil with aluminium guard foils were, after the residual uranium activity had

been counted, positioned at the centre of the double-fission chamber (same position occupied by foils in  $^{140}\text{La}$  measurement) between the two electrodeposited foils (described in Section 4.3.2). Details of the double-fission chamber and foil positions are shown in Figure 13. After foil loading, the double-fission chamber was placed inside a cadmium sleeve to enhance the ratio of fissions in  $^{238}\text{U}$  to fissions in  $^{235}\text{U}$ , then inserted to the 'fully in' position of the pneumatic facility and the foils irradiated for the standard time of two hours in a neutron flux of  $2 \times 10^9$  n/cm<sup>2</sup>/sec. During the irradiation the fission rates from the natural and depleted uranium electrodeposited foils were simultaneously recorded on separate counting systems. At the end of the two hour irradiation the 'standard' foils were allowed to 'cool' before being removed from the fission chamber. Gamma ray counting of the two foils was then done as for the cluster irradiations, that is with a total 'cooling' time of three hours and discriminator setting equivalent to 0.75 MeV. To check that the counting characteristics were similar for both sides of the chamber, the electrodeposited foils were interchanged and measurement of the fission rates repeated. For this repeat measurement the standard uranium foils were also in position. Agreement between the chambers was good and a mean value was determined for the fission rate from the respective foils.

From the fission counting, the fission ratio  $F$  (Section 3) was determined and from the integral gamma counting,  $\gamma'(t)$  was deduced.  $P(t)$  was then determined from Equation (4) and is shown in Table 2.

As an additional check, the fission ratio  $F$  was determined using the technique of fission track counting (Gold and Armani, 1968). A thin slice of mica was placed in contact with the depleted electrodeposited uranium foil and both placed in the double-fission chamber and irradiated in the pneumatic facility. During the irradiation fission fragments from the uranium penetrated the surface of the mica. After irradiation, the mica was removed from the chamber and etched in hydrofluoric acid, whereupon the fission tracks in the mica became visible when viewed under a low power microscope. The number of tracks on the mica was counted and hence the fission rate determined.

The experiment was repeated for the natural electrodeposited uranium foil. The reactor power for these measurements must be chosen to enable the observer to resolve tracks, and hence must be lower for the natural uranium than for the depleted uranium electrodeposited foil. Gold foils were used to monitor the two power levels.

From the ratio of the tracks in the respective mica foils and after correcting for the different power levels used,  $F$  was found to be  $0.851 \pm 0.018$

which is in good agreement with the value of  $0.847 \pm 0.002$  determined by the double-fission chamber measurements.

### 5.2.5 P(t) results

As stated in Section 3, P(t) depends on many variables. With the exception of counter characteristics, these variables are identical for both the NaI and the Ge(Li) counting systems, hence the difference in the P(t) values assigned to the respective systems is due to the different counting characteristics of these systems.

P(t) values for the Ge(Li) systems were measured as  $1.357 \pm 0.043$  and  $1.365 \pm 0.023$  by the  $^{140}\text{La}$  method and the double-fission chamber methods respectively. This agreement is excellent and the weighted mean value  $P(t) = 1.363 \pm 0.021$  and was used to derive  $\delta_{28}$  values for all the Ge(Li) data.

The value of P(t) for the NaI counting system, measured by the  $^{140}\text{La}$  technique only, was  $1.058 \pm 0.047$ .

## 6. DETERMINATION OF $^{235}\text{U}$ CONTENT OF FOIL

The  $^{235}\text{U}$  contents of the natural and the depleted uranium foils are required to determine the parameters a and S of Equation (2). The value assigned to the  $^{235}\text{U}$  content of the natural uranium foils was 7212 ppm  $^{235}\text{U}$  by atoms as given by the N.B.S. ASTM Round Robin Test (1966). The value assigned to the  $^{235}\text{U}$  content of the depleted uranium foils was determined by the method of solid source mass spectrometry and also by the technique of integral gamma-counting after thermal neutron irradiation.

### 6.1 Mass Spectrometer Measurements

Four depleted uranium foils were randomly chosen from the fifty foils used in the  $\delta_{28}$  measurements. These four foils were separately dissolved in  $\text{HNO}_3$  and solutions prepared for mass spectrometer analysis. A standard method (King and Finley 1965) of  $^{235}\text{U}$  absolute analysis was followed. Table 3 lists the depletion values obtained for the four foils. From these four measurements the mean value was taken as  $395 \pm 8$  ppm atoms  $^{235}\text{U}$ .

### 6.2 Thermal Column Measurements

Depletion measurements were made by irradiating pairs of natural uranium and depleted uranium foils in the thermal column of MOATA and then counting the foil activities above selected discriminator levels in a manner similar to that described in Section 5.1. The two experimental arrangements, A and B, used for the irradiation of the uranium foil pairs in the thermal column are shown in Figure 16. By using arrangement A, the depleted uranium foil was exposed to a higher neutron flux than the natural uranium foil so that when both were counted after the irradiation the integral count rates from each foil were approximately

equal. During the irradiation, gold foils 0.025 mm thick were used to monitor the neutron flux at the uranium foil positions.

Arrangement B avoids the use of monitor foils. Here both depleted and natural uranium foils were exposed to the same neutron flux. The resulting count rates were therefore in direct proportion to the depletion, namely about 20:1. Choice of reactor power level for this irradiation was therefore a compromise between an adequate count rate on the depleted foil without being unduly high on the natural one.

From a comparison of the integral gamma-count rates on the respective foils, the  $^{235}\text{U}$  content of the depleted uranium was determined relative to that of natural uranium. Using the N.B.S. value for natural uranium and making the necessary corrections for foil masses, neutron flux perturbation and gamma self shielding, the results shown in Table 3 were obtained for the  $^{235}\text{U}$  content of the depleted uranium foils. The mean result is  $403.2 \pm 1.5$  ppm atoms  $^{235}\text{U}$ .

The foils were counted at different discriminator bias levels, but no significant change in the results of depletion measurement were observed (Table 4). This result is, of course, also relevant to the choice of discriminator level in the cluster irradiation foil gamma-counting.

#### 6.2.1 Intercalibration of depleted uranium foils

The twelve depleted uranium foils used in the  $\delta_{28}$  measurements were made from the same stock material in two batches. Six foils chosen at random from each batch were positioned around the perimeter of a six inch perspex disc and the disc rotated in a well thermalised region in the reactor MOATA. After irradiation, the active foils were gamma-counted. The usual corrections for mass and foil thickness were made and the results compared. Figure 17 shows that the  $^{235}\text{U}$  content is the same for all the depleted uranium foils.

#### 6.3 Summary of $^{235}\text{U}$ Content Measurements for Depleted Uranium Foils

The uranium  $^{235}\text{U}$  content is the same for all depleted foils. Mass spectrometer measurements and reactor thermal column activation measurements gave values of  $395 \pm 8$  ppm and  $403 \pm 2$  ppm atoms  $^{235}\text{U}$  respectively. In view of possible systematic errors in these different methods of determination we have elected to assign equal weight to each of these results rather than take a weighted mean. The value of  $399 \pm 4$  ppm atom  $^{235}\text{U}$  has therefore been adopted as the best estimate. The values of  $a$  and  $S$  thus become 0.9932 and  $0.05494 \pm 0.00056$  respectively. The error in  $a$  is not significant.

#### 6.4 Measurements of Mass Ratio of Electrodeposited Foils

A measurement of the effective ratio of the natural uranium deposited

foil mass to the depleted uranium deposited foil mass determines the correction factor  $M$  used in Equation (4). This measurement was made by irradiating the double-fission chamber, containing the electrodeposited foils in the thermal column of MOATA. During the irradiation the  $^{235}\text{U}$  fission rate from each foil was counted and the ratio,  $f$ , formed of the  $^{235}\text{U}$  fissions from the natural uranium electrodeposited foil and the  $^{235}\text{U}$  fissions from the depleted uranium electrodeposited foil. From this ratio the correction factor

$M = \frac{E_d}{fE_n}$  is found, where  $E_d$  is the  $^{235}\text{U}$  content of the depleted uranium, and  $E_n$  is the  $^{235}\text{U}$  content of the natural uranium. Using the  $^{235}\text{U}$  content values quoted in Sections 6.2 and 6.3, the correction factor  $M$  was found to be  $0.5031 \pm 0.0057$ .

From these measurements, the thickness of the electrodeposited uranium films was estimated as  $191 \mu\text{g}/\text{cm}^2$  and  $100 \mu\text{g}/\text{cm}^2$  for the depleted and natural foils respectively. Using these foils, the detector efficiency can be approximated by  $E = 1 - \frac{\mu}{2R}$  where  $\mu$  is foil thickness in  $\text{mg}/\text{cm}^2$  and  $R$  is mean range of fission fragments in uranium (assumed here as  $\sim 10 \text{ mg}/\text{cm}^2$ ). Hence for the foils used in the fission counting, approximately 99 per cent of the fragments were detected.

## 7. ERRORS

The following sources of error in the measurement of  $\delta_{28}$  have been considered.

### (a) Counting Statistics

In normal circumstances, sufficient counts were always taken to ensure that this contribution to the error in  $\delta_{28}$  did not exceed  $\pm 0.5$  per cent.

### (b) Air Background

This was monitored at regular intervals during foil counting, and contributed only of the order  $\pm 0.2$  per cent to the uncertainty in the corrected count-rates.

### (c) Natural Activity of Uranium Foils

This was measured for each foil before an irradiation. The contribution to the error in corrected count-rate was again small ( $\pm 0.02$  per cent).

### (d) Dead Time Losses

The Ge(Li) system compensated automatically for dead time corrections. The effective dead time for the NaI system was about  $18 \mu\text{s}$ . However, as the counting rates never exceeded  $2000 \text{ c/s}$ , the uncertainty of the effect of dead time was small ( $\pm 0.4$  per cent).

### (e) $^{140}\text{La}$ Peak Estimation

It was estimated that the background subtraction technique adopted

resulted in uncertainties of  $\pm 0.4$  per cent in the residual count-rates under the  $^{140}\text{La}$  peak.

(f) Gap Corrections

The uranium foils and aluminium covers form a perturbing gap in the fuel rod for which some correction should be made. For similar  $\text{UO}_2$  fuel clusters, de Lange et al. (1966) were unable to detect gap effects experimentally. Nevertheless, we have applied a gap effect correction using the method of Bigham (1965) which, in these measurements, amounts to about 0.5 per cent. An uncertainty of  $\pm 0.5$  per cent has been assigned to  $\delta_{28}$  values for this correction.

(g) Gamma Ray Self Shielding

No correction was necessary as the foil pairs were always selected to be of the same thickness and the ratio formed tends to cancel out these effects (Bigham 1965).

(h)  $^{235}\text{U}$  Content of Foils

Uncertainty in the  $^{235}\text{U}$  content of the foils used in the measurements produces a direct systematic error in the  $\delta_{28}$  results. The measurements summarised in Section 6.3 indicate an uncertainty of  $\pm 1$  per cent in the  $^{235}\text{U}$  content of the depleted foils. The associated uncertainty in  $\delta_{28}$  is up to  $\pm 2$  per cent.

(i) P(t) Determination

The ratio of the fission yields introduces an error of  $\pm 2.8$  per cent into the  $^{140}\text{La}$  determination of P(t) for both the NaI and the Ge(Li) systems. However when combined with statistical errors the errors in P(t) for the NaI and the Ge(Li) systems are  $\pm 4.4$  per cent and  $\pm 3.2$  per cent respectively.

The double-fission chamber method used for the Ge(Li) system only, gave an experimental precision of  $\pm 1.7$  per cent in P(t) and systematic errors associated with this method as used are believed to be small. Furthermore, the result is in excellent agreement with the  $^{140}\text{La}$  P(t). It therefore seems unlikely that the error in P(t) including unknown systematic uncertainties can be worse than the  $\pm 3.2$  per cent estimated for the  $^{140}\text{La}$  method and this is the contribution which has been allowed in deriving the error in absolute values of  $\delta_{28}$ .

(j) Additional Errors

A summary of the error contributions discussed above is given in Table 5. However, when values of  $\delta_{28}$  obtained for common ring positions ( $R_2, R_3, R_7, R_8, R_9, R_{11}, R_{12}$ ) were examined, it was found that their spread was much greater than would be expected from compounding the error contributions

considered above, and corresponded to a standard deviation of some  $\pm 4$  per cent on an individual result.

It was concluded that some undetected source of random error must have been present in the experimental routine, or that some of the contributions considered have been underestimated.

The errors given in Tables 6a, 6b and 6c include allowance for the observed spread.

## 8. $\delta_{28}$ RESULTS

The integral gamma-count data collected by the NaI counting system and by the Ge(Li) counting system for the foils irradiated in each cluster position were analysed by a computer program BARC (Rose 1969) which calculated the ratios  $\gamma(t)$ .

A second program DEL28 (Rose 1969) combined the measured  $\gamma(t)$  ratios with the measured  $P(t)$  values (Table 1) and derived values of  $\delta_{28}$  for each rod position in the respective cluster and also a mean value of  $\delta_{28}$  for the particular cluster. The flow diagram in Figure 18 shows the steps followed in determining the  $\delta_{28}$  values.

Tables 6a, 6b, give all measured values of  $\delta_{28}$  for the Ge(Li) and NaI methods respectively. Table 6c results are the weighted mean of those in Tables 6a and 6b. The final column (5) of Table 6a gives the Ge(Li) cluster averaged fission ratio for each cluster. This quantity is not given for the NaI data (Table 6b) since the  $^{235}\text{U}$  fission rate variation across the cluster was not available from the NaI measurements. However the final column (5) of Table 6c was derived by combination of the Ge(Li) and NaI data in the manner shown at the foot of the table.

## 9. SUMMARY AND CONCLUSION

In summary, the following points are made:

(1) Measurements of  $\delta_{28}$  have been made in a range of geometries and coolant densities for  $\text{UO}_2$  rod clusters with an overall accuracy of about 4.5 per cent.

(2) The use of polystyrene to simulate reduced density  $\text{H}_2\text{O}$  for fast neutron spectrum events has proved highly successful. The ease with which the material could be moulded to produce complicated geometries to the close tolerances required, eliminated many of the problems initially envisaged in trying to simulate low density  $\text{H}_2\text{O}$ .

(3) In the  $P(t)$  calibration measurements, both the  $^{140}\text{La}$  and the double-fission chamber techniques have been used. As stated by Wolberg et al. (1964) the  $^{140}\text{La}$  method to measure  $\delta_{28}$  offers all the advantages of direct measurement,

but at present the uncertainty in the ratio of the  $^{140}\text{Ba}$  yield from  $^{235}\text{U}$  fission to the  $^{140}\text{Ba}$  yield from  $^{238}\text{U}$  fission, limits the accuracy of this technique. Therefore, until the  $^{140}\text{Ba}$  yield ratios are known with more certainty, the double-fission chamber technique appears to be more accurate.

(4) Using the value of yield ratio reported by Ciuffolotti (1968), the  $P(t)$  values measured by the  $^{140}\text{La}$  method were in excellent agreement with the double-fission chamber techniques.

(5) With regard to the variation of  $P(t)$  with time we have found that under the conditions of these experiments a constant value of  $P(t)$  can be assumed. Evidence for this is given in Figure 20 which shows there is little variation of the ratio of depleted and natural foil activities with time. Further support is given by Konishi and Yamamoto (1969) who show the effects of bias level and choice of counting time on  $P(t)$  values.

(6) Accurate determination of the enrichment of the depleted foils is important as  $\pm 1$  per cent error in enrichment gives up to  $\pm 2$  per cent uncertainty in  $\delta_{28}$ .

(7) The plots (Figure 19) of cluster averaged  $\delta_{28}$  versus 'coolant' hydrogen atom density show some tendency for the  $\delta_{28}$  values to pass through a maximum corresponding to the lower density polystyrene 'coolant'. The exception is the wide spaced 19-rod cluster. The effect may not be significant, but if it is real, it can possibly be explained by the polystyrene in the close packed clusters being appreciably thicker between the outer ring of rods and the housing tube than between the rods of the inner rings. When the low density polystyrene is used, additional fissions by neutrons scattered back into the fuel region from the outer layer of polystyrene may outweigh the reduction due to the very small total quantity of hydrogen between the cluster rods.

#### 10. ACKNOWLEDGEMENTS

Many individuals contributed to this experiment. Mr. M. Srinivasan and Mr. D.B. McCulloch proposed the experimental programme. Members of the R.E.D. Physics Division assisted in the foil counting and Mr. L. Srinivasan ran many computer programs. The staff of BARC workshops fabricated the cluster components and made the necessary modifications to the ZERLINA reactor.

Mr. A.H. Mistry provided the electronics used for the NaI counting system. The polystyrene moulds were manufactured by R. Farmer and D. Hyde of AAEC. In this context, the technical advice of Mr. P. Burmester of BASF Australia, is much appreciated. Messrs. A.M. Beech, J. Eberhardt and A.J. Tavendale supplied the germanium detector and preamplifier. Mr. E. Lippa carried out the mass

considered above, and corresponded to a standard deviation of some  $\pm 4$  per cent on an individual result.

It was concluded that some undetected source of random error must have been present in the experimental routine, or that some of the contributions considered have been underestimated.

The errors given in Tables 6a, 6b and 6c include allowance for the observed spread.

## 8. $\delta_{28}$ RESULTS

The integral gamma-count data collected by the NaI counting system and by the Ge(Li) counting system for the foils irradiated in each cluster position were analysed by a computer program BARC (Rose 1969) which calculated the ratios  $\gamma(t)$ .

A second program DEL28 (Rose 1969) combined the measured  $\gamma(t)$  ratios with the measured  $P(t)$  values (Table 1) and derived values of  $\delta_{28}$  for each rod position in the respective cluster and also a mean value of  $\delta_{28}$  for the particular cluster. The flow diagram in Figure 18 shows the steps followed in determining the  $\delta_{28}$  values.

Tables 6a, 6b, give all measured values of  $\delta_{28}$  for the Ge(Li) and NaI methods respectively. Table 6c results are the weighted mean of those in Tables 6a and 6b. The final column (5) of Table 6a gives the Ge(Li) cluster averaged fission ratio for each cluster. This quantity is not given for the NaI data (Table 6b) since the  $^{235}\text{U}$  fission rate variation across the cluster was not available from the NaI measurements. However the final column (5) of Table 6c was derived by combination of the Ge(Li) and NaI data in the manner shown at the foot of the table.

## 9. SUMMARY AND CONCLUSION

In summary, the following points are made:

(1) Measurements of  $\delta_{28}$  have been made in a range of geometries and coolant densities for  $\text{UO}_2$  rod clusters with an overall accuracy of about 4.5 per cent.

(2) The use of polystyrene to simulate reduced density  $\text{H}_2\text{O}$  for fast neutron spectrum events has proved highly successful. The ease with which the material could be moulded to produce complicated geometries to the close tolerances required, eliminated many of the problems initially envisaged in trying to simulate low density  $\text{H}_2\text{O}$ .

(3) In the  $P(t)$  calibration measurements, both the  $^{140}\text{La}$  and the double-fission chamber techniques have been used. As stated by Wolberg et al. (1964) the  $^{140}\text{La}$  method to measure  $\delta_{28}$  offers all the advantages of direct measurement,

but at present the uncertainty in the ratio of the  $^{140}\text{Ba}$  yield from  $^{235}\text{U}$  fission to the  $^{140}\text{Ba}$  yield from  $^{238}\text{U}$  fission, limits the accuracy of this technique. Therefore, until the  $^{140}\text{Ba}$  yield ratios are known with more certainty, the double-fission chamber technique appears to be more accurate.

(4) Using the value of yield ratio reported by Ciuffolotti (1968), the  $P(t)$  values measured by the  $^{140}\text{La}$  method were in excellent agreement with the double-fission chamber techniques.

(5) With regard to the variation of  $P(t)$  with time we have found that under the conditions of these experiments a constant value of  $P(t)$  can be assumed. Evidence for this is given in Figure 20 which shows there is little variation of the ratio of depleted and natural foil activities with time. Further support is given by Konishi and Yamamoto (1969) who show the effects of bias level and choice of counting time on  $P(t)$  values.

(6) Accurate determination of the enrichment of the depleted foils is important as  $\pm 1$  per cent error in enrichment gives up to  $\pm 2$  per cent uncertainty in  $\delta_{28}$ .

(7) The plots (Figure 19) of cluster averaged  $\delta_{28}$  versus 'coolant' hydrogen atom density show some tendency for the  $\delta_{28}$  values to pass through a maximum corresponding to the lower density polystyrene 'coolant'. The exception is the wide spaced 19-rod cluster. The effect may not be significant, but if it is real, it can possibly be explained by the polystyrene in the close packed clusters being appreciably thicker between the outer ring of rods and the housing tube than between the rods of the inner rings. When the low density polystyrene is used, additional fissions by neutrons scattered back into the fuel region from the outer layer of polystyrene may outweigh the reduction due to the very small total quantity of hydrogen between the cluster rods.

#### 10. ACKNOWLEDGEMENTS

Many individuals contributed to this experiment. Mr. M. Srinivasan and Mr. D.B. McCulloch proposed the experimental programme. Members of the R.E.D. Physics Division assisted in the foil counting and Mr. L. Srinivasan ran many computer programs. The staff of BARC workshops fabricated the cluster components and made the necessary modifications to the ZERLINA reactor.

Mr. A.H. Mistry provided the electronics used for the NaI counting system. The polystyrene moulds were manufactured by R. Farmer and D. Hyde of AAEC. In this context, the technical advice of Mr. P. Burmester of BASF Australia, is much appreciated. Messrs. A.M. Beech, J. Eberhardt and A.J. Tavendale supplied the germanium detector and preamplifier. Mr. E. Lippa carried out the mass

spectrometer measurements. Finally, we wish to thank Mrs. E.K. Rose who wrote and ran the computer programs required for the analysis of the results.

11. REFERENCES

- A.S.T.M. Round Robin Test (Jan 1966) - National Bureau of Standards.  
Bigham, C.B. (1965) - CRRP1220.  
Ciuffolotti, L. (1968) - Energia Nucleare 15, 272.  
de Lange, P.W., Bigham, C.B., Green, R.E., and Manuel, T.J. (1966) -  
AECL/2636.  
Gold, R. and Armani, R.J. (1968) - Nucl. Sci. and Eng. 34, 13.  
King, W.F. and Finley, H.O. (1965) - NBL/216.  
Konishi, T. and Yamamoto, H. (1969) - Journal of Nuclear Sci. and  
Technology. 6, 243.  
Marks, A.P. (1962) - Atomic Energy in Australia (October), 9.  
Mistry, A.H. (1968) - RED/ERP/Note 50.  
Probhakar, B.S., Lakshmanachar, N., Deniz, V.C. and Soman, S.D. (1962) -  
AEET/RC/CE-1.  
Rose, A. (1970) - Nuclear Instruments and Methods, 77, 167.  
Rose, E.K. (1969) - AAEC RP/CP72.  
Wolberg, J.R., Thompson, T.J. and Kaplan, I. (1964) - STI/Pub/79, 11, 147.

6

0

TABLE 1  
MULTI-ROD CLUSTERS AND CLUSTER COOLANTS  
USED IN FAST FISSION MEASUREMENTS

Cluster	Coolant			
7 Exp.	Air	-	-	H <sub>2</sub> O
7	Air	0.25 g/cm <sup>3</sup> polystyrene	0.64 g/cm <sup>3</sup> polystyrene	H <sub>2</sub> O
19 Exp.	Air	0.25 g/cm <sup>3</sup> polystyrene	0.64 g/cm <sup>3</sup> polystyrene	H <sub>2</sub> O
19	Air	0.25 g/cm <sup>3</sup> polystyrene	0.64 g/cm <sup>3</sup> polystyrene	H <sub>2</sub> O
37	Air	0.25 g/cm <sup>3</sup> polystyrene	0.64 g/cm <sup>3</sup> polystyrene	H <sub>2</sub> O
61	Air	-	-	H <sub>2</sub> O

TABLE 2  
COMPARISON OF P(t) VALUES

Measurement	System	Counting Interval	Bias	P(t)
<sup>140</sup> La	NaI	180 min - 360 min	0.75 MeV	1.058 ± 0.047
<sup>140</sup> La	Ge(Li)	180 min - 360 min	0.75 MeV	1.357 ± 0.043
Double-Fission Chamber	Ge(Li)	180 min - 360 min	0.75 MeV	1.365 ± 0.023

TABLE 3

MASS SPECTROMETER MEASUREMENTS

Foil	Number of Scans	Depletion ppm	Depletion Corrected for NBS U-500 Standard
1	130	404	399
2	120	403	398
3	104	396	391
4	30	398	383

TABLE 4

DEPLETED URANIUM FOIL ENRICHMENT

Foil	Bias (MeV)	Arrangement	Enrichment (ppm) *
1	0.73	A	405
2	0.55	A	410
3	0.55	A	403
3	0.73	A	400 401
3	1.03	A	400
4	0.75	B	402
5	1.25	B	400
6	1.25	B	401

\* Note: all measured values are atom per cent  
mean value for enrichment is  $403 \pm 1.5$  ppm

TABLE 5

ERRORS IN THE MEASUREMENT OF  $\delta_{28}$

Source of Error	Ge(Li)		NaI
	$^{140}\text{La}$	D.F.C.	$^{140}\text{La}$
Counting statistics	$\pm 0.5\%$	$\pm 0.5\%$	$\pm 0.4\%$
Air background	-	$\pm 0.02\%$	$\pm 0.02\%$
Natural activity on uranium foils	$< 0.01\%$	$\pm 0.02\%$	$\pm 0.02\%$
Dead time losses	$\pm 0.01\%$	$\pm 0.01\%$	$\pm 0.04\%$
Peak isolation	$\pm 0.4\%$	-	$\pm 0.5\%$
Gap corrections	$\pm 0.5\%$	$\pm 0.5\%$	$\pm 0.5\%$
Gamma ray self shielding	Nil	Nil	Nil
$^{140}\text{La}$ P(t) determination	$\pm 2.8\%$	-	$\pm 4.4\%$
D.F.C. P(t) determination	-	$\pm 2\%$	-
$^{235}\text{U}$ content	$\pm 1\%$	$\pm 1\%$	$\pm 1\%$

TABLE 6a

PAST FISSION RATIOS IN CLUSTERS (Ge/Li RESULTS)

1	2	3										4	5
		Rod US Ratios											
Cluster	Coolant	R1	R2	R3	R4	R7	R8	R9	R11	R12	Cluster* Averaged US Ratio US	Cluster Average US** Cluster Average US	
Exp. 7-Rod	Air	0.0301 ± 14	0.0258 ± 13	0.0243 ± 13							0.0258 ± 11	0.0257 ± 11	
	H <sub>2</sub> O	0.0310 ± 17	0.0211 ± 14	0.0193 ± 14							0.0217 ± 11	0.0214 ± 11	
7-Rod	Air	0.0398 ± 16	0.0297 ± 13	0.0306 ± 14							0.0315 ± 12	0.0314 ± 12	
	L.D.	0.0381 ± 16	0.0332 ± 14	0.0297 ± 14							0.0324 ± 12	0.0322 ± 12	
	H.D.	0.0393 ± 16	0.0266 ± 15	0.0309 ± 14							0.0303 ± 12	0.0302 ± 12	
	H <sub>2</sub> O	0.0419 ± 19	0.0299 ± 15	0.0307 ± 15							0.0320 ± 13	-	
Exp. 19-Rod	Air	0.0472 ± 19		0.0474 ± 19	0.0358 ± 15						0.0401 ± 15	0.0398 ± 15	
	L.D.	0.0523 ± 20		0.0424 ± 17	0.0315 ± 14						0.0360 ± 14	0.0354 ± 14	
	H.D.	0.0533 ± 22		0.0486 ± 21	0.0282 ± 14						0.0360 ± 15	0.0343 ± 14	
	H <sub>2</sub> O	0.0528 ± 21		0.0507 ± 21	0.0283 ± 14						0.0366 ± 15	0.0344 ± 14	
19-Rod	Air	0.0594 ± 25		0.0570 ± 24	0.0406 ± 18						0.0467 ± 18	0.0462 ± 18	
	L.D.	0.0685 ± 25		0.0609 ± 23	0.0415 ± 17						0.0491 ± 18	0.0478 ± 18	
	H.D.	0.0703 ± 25		0.0590 ± 22	0.0393 ± 16						0.0471 ± 17	0.0455 ± 16	
	H <sub>2</sub> O	0.0674 ± 27		0.0605 ± 24	0.0377 ± 17						0.0465 ± 18	0.0445 ± 17	
37-Rod	Air	0.0926 ± 32		0.0867 ± 31	0.0769 ± 27	0.0496 ± 19	0.0484 ± 19				0.0654 ± 22	0.0631 ± 21	
	L.D.	0.0934 ± 33		0.0896 ± 36	0.0784 ± 32	0.0455 ± 21	0.0497 ± 22				0.0656 ± 25	0.0621 ± 23	
	H.D.	0.1058 ± 37		0.0948 ± 37	0.0751 ± 29	0.0432 ± 18	0.0452 ± 19				0.0641 ± 23	0.0590 ± 21	
	H <sub>2</sub> O	0.1028 ± 41		0.0993 ± 38	0.0726 ± 28	0.0388 ± 23	0.0309 ± 20				0.0594 ± 26	0.0519 ± 23	
61-Rod	Air	0.1302 ± 45		0.1284 ± 46	0.1149 ± 41	0.0868 ± 32	0.0815 ± 29	0.0549 ± 22	0.0556 ± 21	0.0567 ± 23	0.0841 ± 28	0.0781 ± 26	
	H <sub>2</sub> O	0.1442 ± 51		0.1436 ± 56	0.0981 ± 38	0.0681 ± 27	0.0709 ± 29	0.0380 ± 18	0.0426 ± 19	0.0439 ± 19	0.0726 ± 26	0.0609 ± 22	

Note: Errors are in units of 10<sup>-4</sup>

\*Cluster Average =  $\frac{1}{n}(A_0 + 6A_1 + 12A_2 + 18A_3 + 24A_4)$  where n is number of rods and A<sub>0</sub> → A<sub>4</sub> is ring number. E.g. 7-rod cluster average =  $\frac{1}{7}(R_1 + 3(R_2 + R_3))$

\*\*See Section 8

TABLE 6b

FAST FISSION RATIOS IN CLUSTERS (NaI RESULTS)

1	2	3											4
		Rod $\frac{US}{US}$ Ratios											
Cluster	Coolant	R1	R2	R3	R4	R7	R8	R9	R11	R12	Cluster Averaged $\frac{US}{US}$ Ratio		
Exp. 7-Rod	Air	0.0307 ± 15	0.0258 ± 13	0.0277 ± 14							0.0273 ± 13		
	H <sub>2</sub> O	0.0298 ± 15	0.0268 ± 14	0.0223 ± 12							0.0253 ± 12		
7-Rod	Air	0.0331 ± 16	0.0317 ± 15	0.0287 ± 14							0.0306 ± 14		
	L.D.	0.0401 ± 19	0.0314 ± 15	0.0324 ± 16							0.0330 ± 15		
	H.D.	0.0407 ± 19	0.0289 ± 15	0.0290 ± 14							0.0307 ± 14		
	H <sub>2</sub> O	0.0383 ± 18	0.0278 ± 14	0.0282 ± 14							0.0295 ± 14		
Exp. 19-Rod	Air	0.0536 ± 25		0.0477 ± 22	0.0386 ± 18						0.0423 ± 20		
	L.D.	0.0515 ± 24		0.0465 ± 22	0.0348 ± 17						0.0393 ± 18		
	H.D.	0.0554 ± 26		0.0477 ± 22	0.0333 ± 16						0.0390 ± 18		
	H <sub>2</sub> O	0.0495 ± 23		0.0417 ± 20	0.0278 ± 14						0.0333 ± 16		
19-Rod	Air	0.0635 ± 29		0.0578 ± 27	0.0413 ± 20						0.0477 ± 22		
	L.D.	0.0678 ± 31		0.0600 ± 28	0.0421 ± 20						0.0491 ± 23		
	H.D.	0.0720 ± 33		0.0589 ± 27	0.0407 ± 19						0.0481 ± 22		
	H <sub>2</sub> O	0.0685 ± 31		0.0593 ± 27	0.0366 ± 18						0.0454 ± 21		
37-Rod	Air	0.0961 ± 43		0.0924 ± 42	0.0768 ± 35	0.0531 ± 25	0.0500 ± 23				0.0676 ± 30		
	L.D.	0.0976 ± 44		0.0890 ± 40	0.0728 ± 38	0.0476 ± 22	0.0446 ± 21				0.0631 ± 30		
	H.D.	0.1019 ± 46		0.0935 ± 43	0.0728 ± 33	0.0444 ± 21	0.0445 ± 21				0.0632 ± 29		
	H <sub>2</sub> O	0.0982 ± 44		0.0897 ± 40	0.0658 ± 30	0.0406 ± 19	0.0405 ± 19				0.0583 ± 26		
61-Rod	Air	0.1262 ± 57		0.1194 ± 54	0.1062 ± 48	0.0851 ± 38	0.0819 ± 37	0.0541 ± 25	0.0497 ± 23	0.0566 ± 26	0.0804 ± 36		
	H <sub>2</sub> O	0.1351 ± 61		0.1214 ± 55	0.1055 ± 48	0.0748 ± 34	0.0772 ± 35	0.0390 ± 19	0.0427 ± 20	0.0396 ± 19	0.0733 ± 33		

Note: Errors are in units of 10<sup>-4</sup>

TABLE 6C

FAST FISSION RATIOS IN CLUSTERS (MEAN OF NaI AND Ge(Li) RESULTS)

1	2	3										4	5
		Rod US Ratios											
Cluster	Coolant	R1	R2	R3	R4	R7	R8	R9	R11	R12	Cluster Averaged US Ratio	See Footnote	
Exp. 7-Rod	Air	0.0304 ± 10	0.0259 ± 9	0.0258 ± 9							0.0264 ± 8	0.0263 ± 11	
	H <sub>2</sub> O	0.0304 ± 11	0.0210 ± 10	0.0240 ± 10							0.0234 ± 8	0.0231 ± 12	
7-Rod	Air	0.0364 ± 11	0.0306 ± 10	0.0297 ± 10							0.0311 ± 9	0.0310 ± 12	
	L.D.	0.0389 ± 12	0.0323 ± 10	0.0308 ± 10							0.0326 ± 10	0.0324 ± 12	
	H.D.	0.0399 ± 12	0.0278 ± 10	0.0300 ± 10							0.0304 ± 9	0.0303 ± 12	
	H <sub>2</sub> O	0.0400 ± 13	0.0288 ± 10	0.0294 ± 10							0.0308 ± 9	0.0308 ± 13	
Exp. 19-Rod	Air	0.0495 ± 15		0.0475 ± 14	0.0370 ± 12						0.0409 ± 12	0.0406 ± 15	
	L.D.	0.0519 ± 15		0.0440 ± 13	0.0328 ± 11						0.0373 ± 11	0.0367 ± 14	
	H.D.	0.0542 ± 16		0.0482 ± 15	0.0304 ± 11						0.0372 ± 12	0.0354 ± 15	
	H <sub>2</sub> O	0.0512 ± 16		0.0459 ± 14	0.0280 ± 10						0.0350 ± 11	0.0329 ± 14	
19-Rod	Air	0.0611 ± 19		0.0573 ± 18	0.0409 ± 13						0.0471 ± 14	0.0466 ± 18	
	L.D.	0.0682 ± 20		0.0605 ± 18	0.0418 ± 13						0.0491 ± 14	0.0478 ± 18	
	H.D.	0.0709 ± 20		0.0590 ± 17	0.0399 ± 12						0.0475 ± 14	0.0459 ± 17	
	H <sub>2</sub> O	0.0678 ± 20		0.0600 ± 18	0.0372 ± 12						0.0460 ± 14	0.0440 ± 17	
37-Rod	Air	0.0939 ± 26		0.0888 ± 25	0.0769 ± 21	0.0509 ± 15	0.0491 ± 15				0.0661 ± 18	0.0638 ± 21	
	L.D.	0.0949 ± 27		0.0892 ± 27	0.0762 ± 24	0.0465 ± 15	0.0470 ± 15				0.0645 ± 18	0.0611 ± 23	
	H.D.	0.1043 ± 29		0.0943 ± 28	0.0741 ± 22	0.0437 ± 14	0.0449 ± 14				0.0637 ± 18	0.0586 ± 21	
	H <sub>2</sub> O	0.1007 ± 30		0.0949 ± 28	0.0694 ± 20	0.0399 ± 15	0.0360 ± 14				0.0588 ± 18	0.0514 ± 23	
61-Rod	Air	0.1286 ± 35		0.1246 ± 35	0.1112 ± 31	0.0861 ± 24	0.0816 ± 23	0.0545 ± 17	0.0529 ± 16	0.0567 ± 17	0.0827 ± 22	0.0768 ± 26	
	H <sub>2</sub> O	0.1405 ± 39		0.1321 ± 39	0.1010 ± 30	0.0707 ± 21	0.0734 ± 22	0.0385 ± 13	0.0426 ± 14	0.0420 ± 13	0.0729 ± 20	0.0611 ± 22	

Note: Errors are in units of 10<sup>-4</sup>.

Column 5 is derived mean cluster average result

i.e. Col 4/6c x Col 5/6a  
Col 4/6a

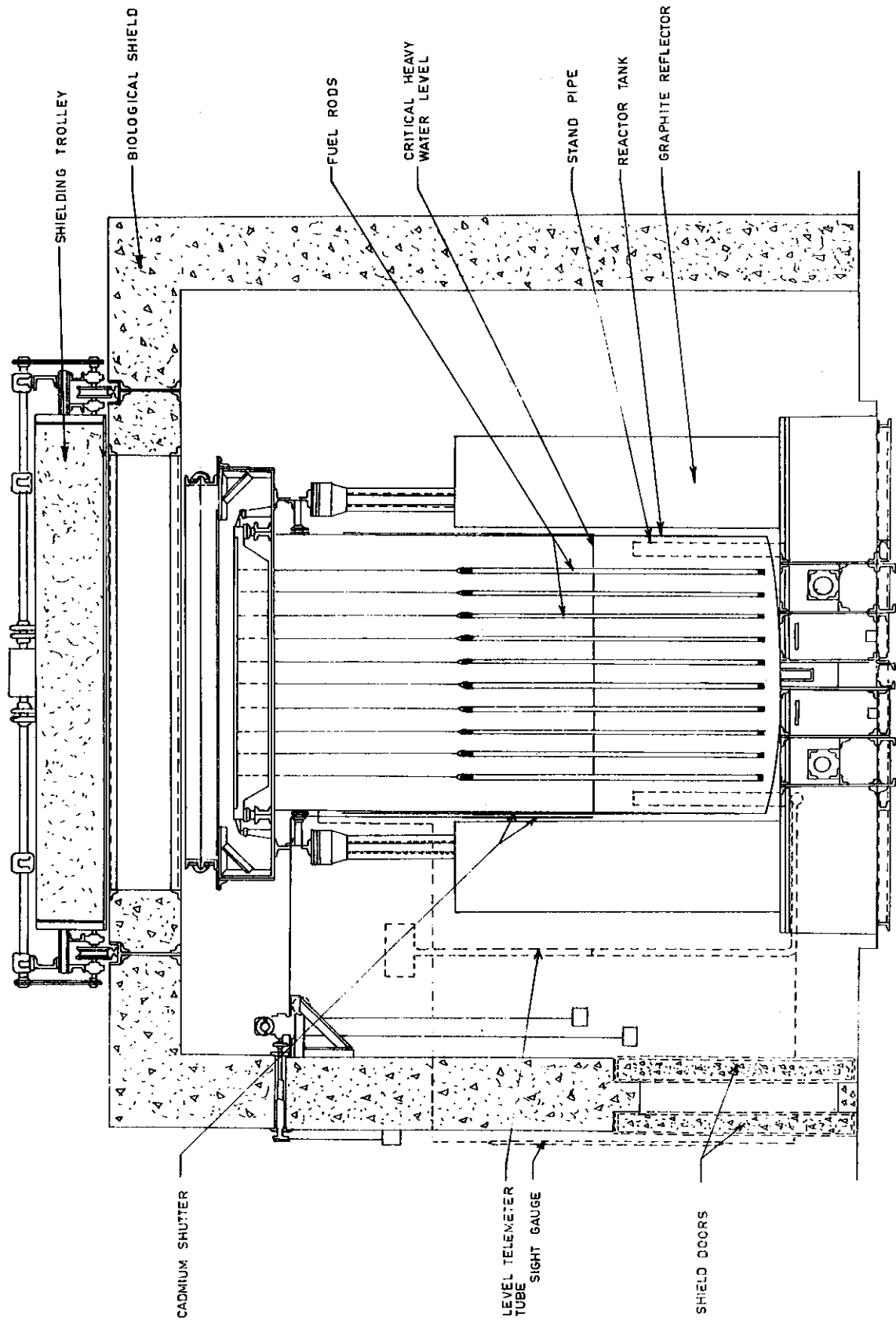


FIGURE 1. VERTICAL CROSS SECTION OF ZERLINA

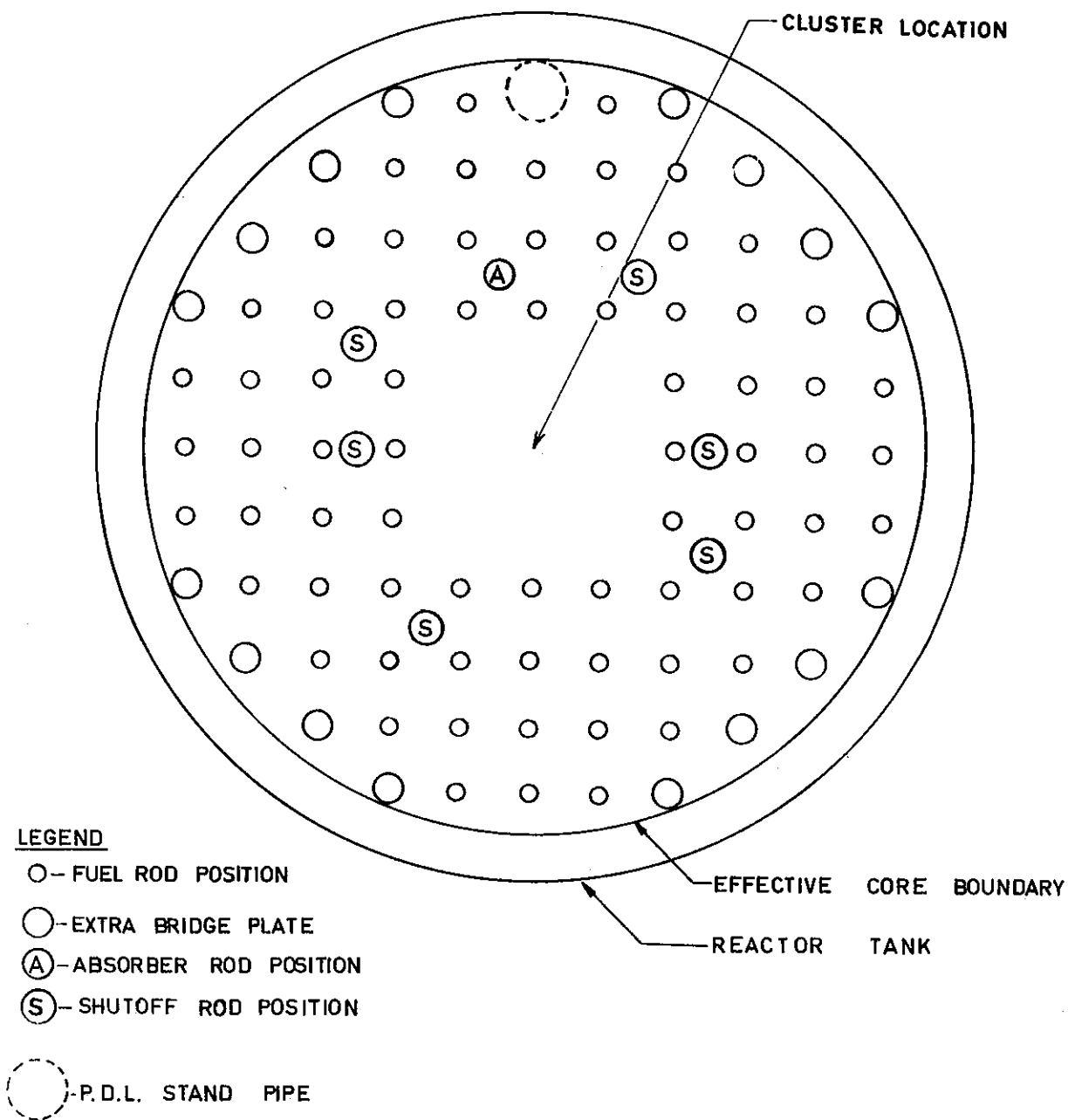


FIGURE 2. CROSS SECTION OF ZERLINA CORE

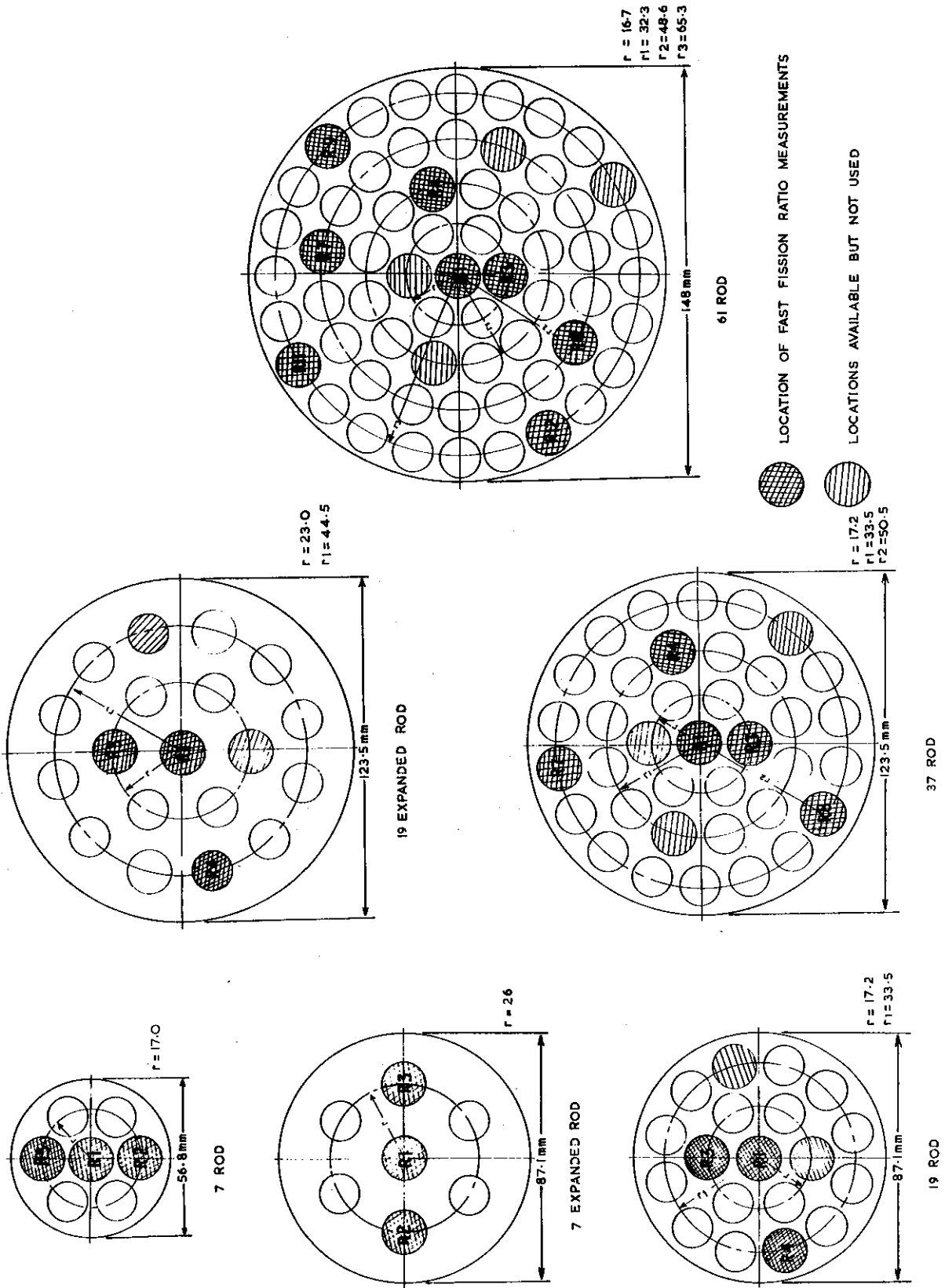


FIGURE 3. CLUSTER DETAILS

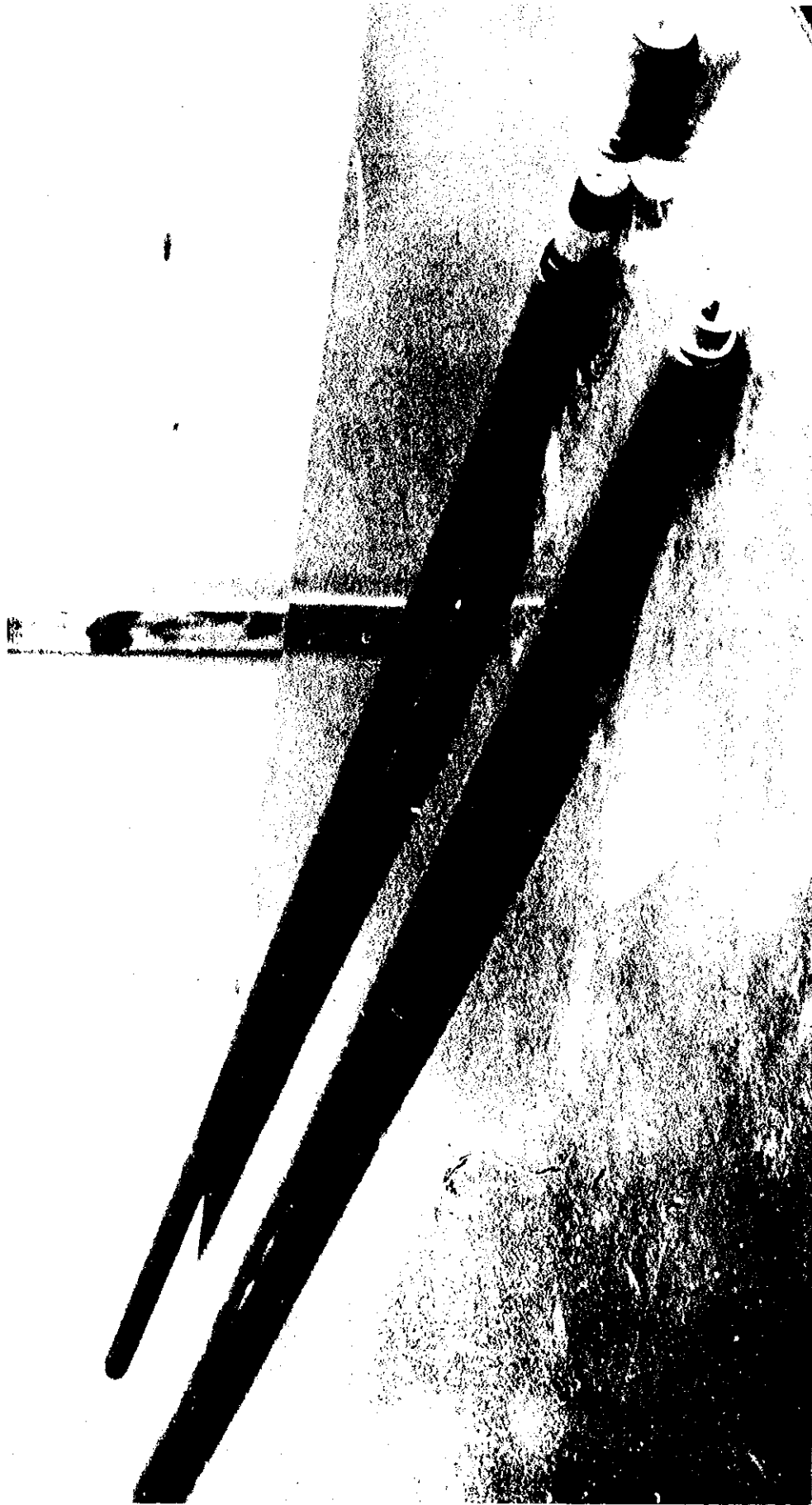


FIGURE 4. DEMOUNTABLE ROD

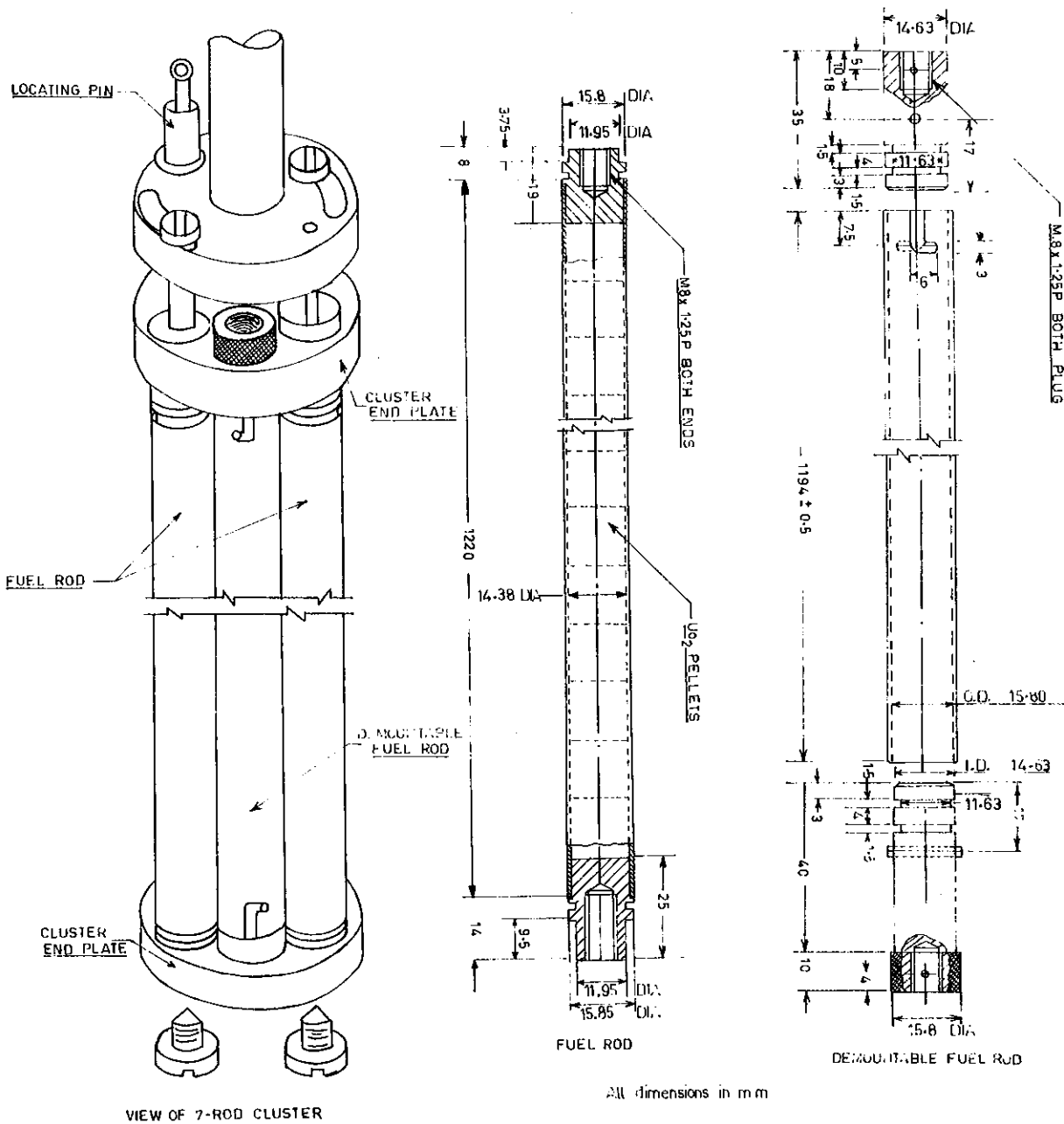


FIGURE 5. DETAILS OF FUEL RODS AND ASSEMBLY OF 7-ROD CLUSTER



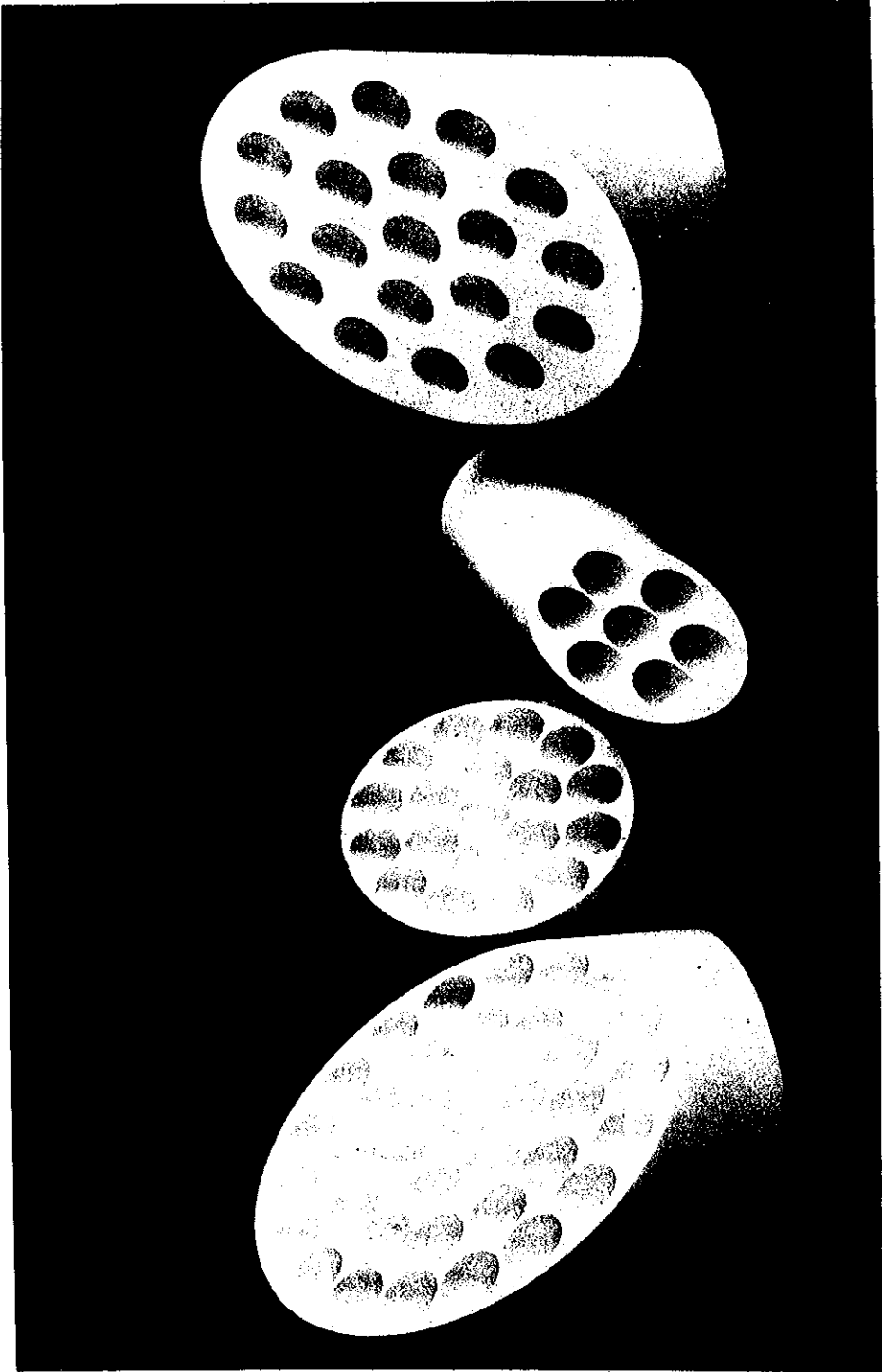


FIGURE 7. CROSS SECTION OF MOULDINGS

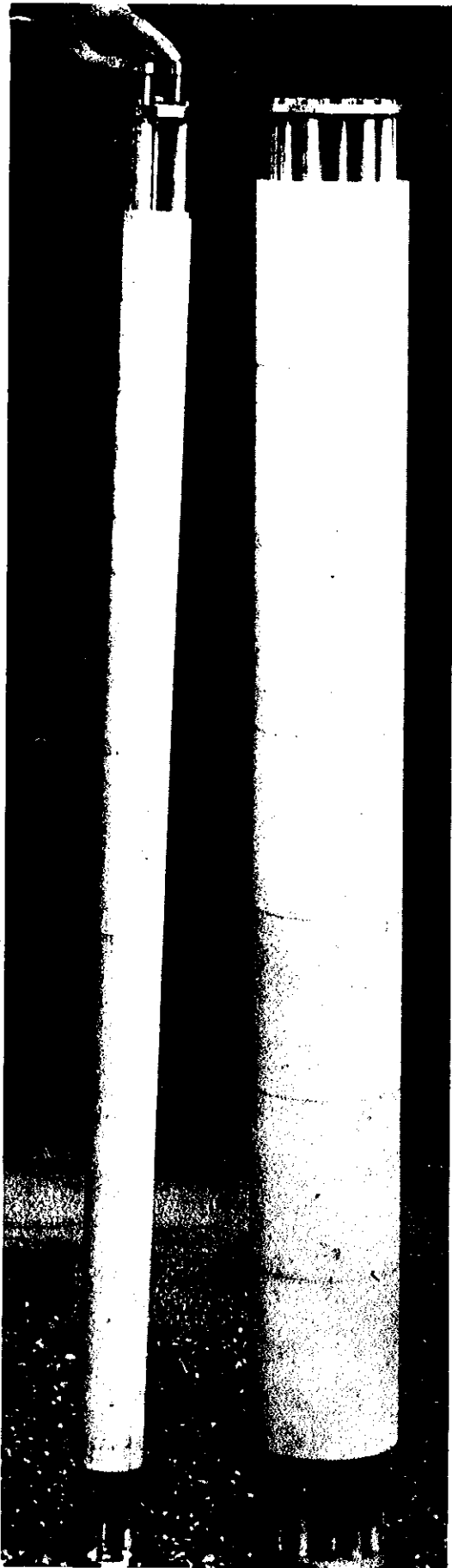


FIGURE 8. 7 AND 19-ROD CLUSTERS



FIGURE 9. 37-ROD CLUSTER WITH HOUSING TUBE

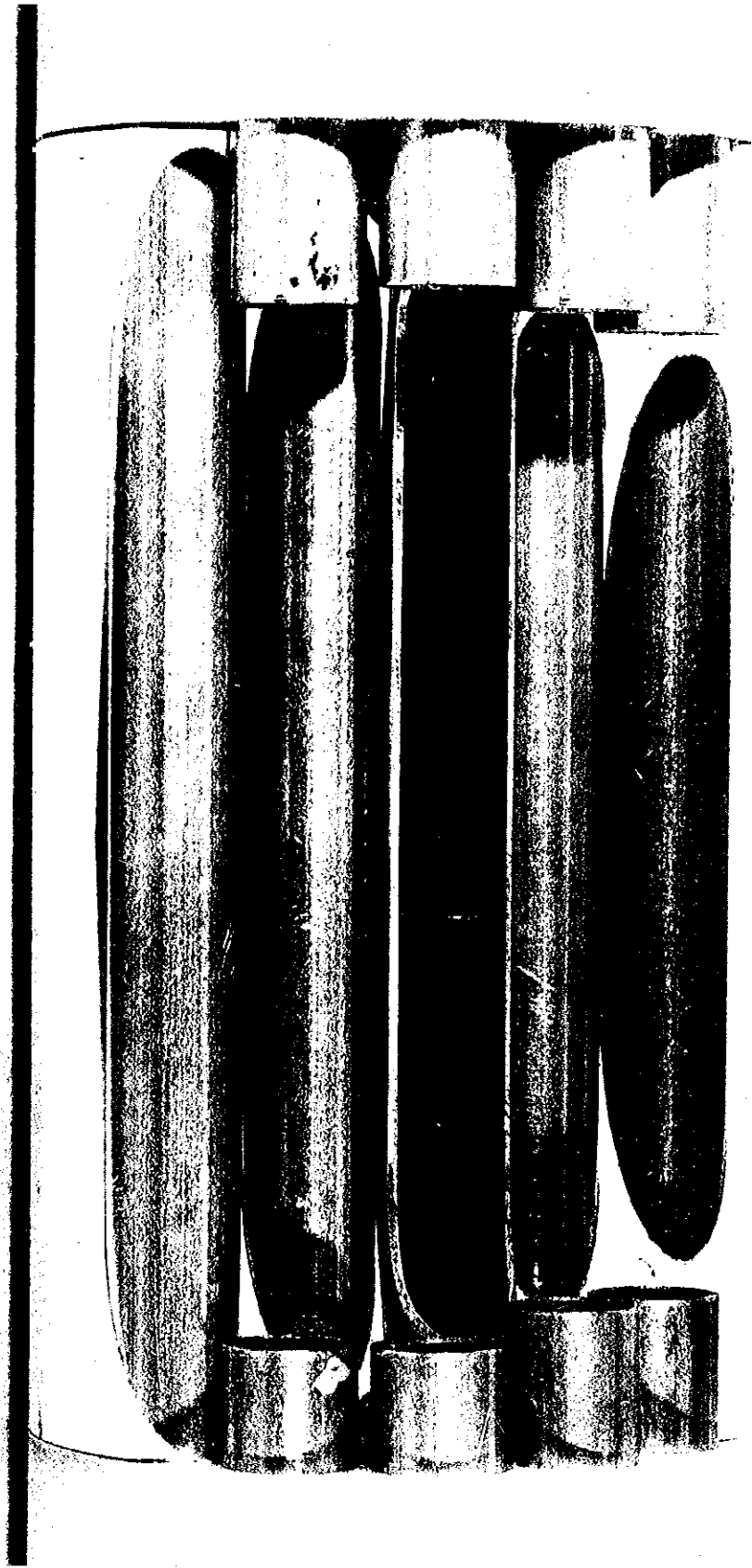


FIGURE 10. SECTION OF 19-ROD CLUSTER SHOWING FOIL PACKET

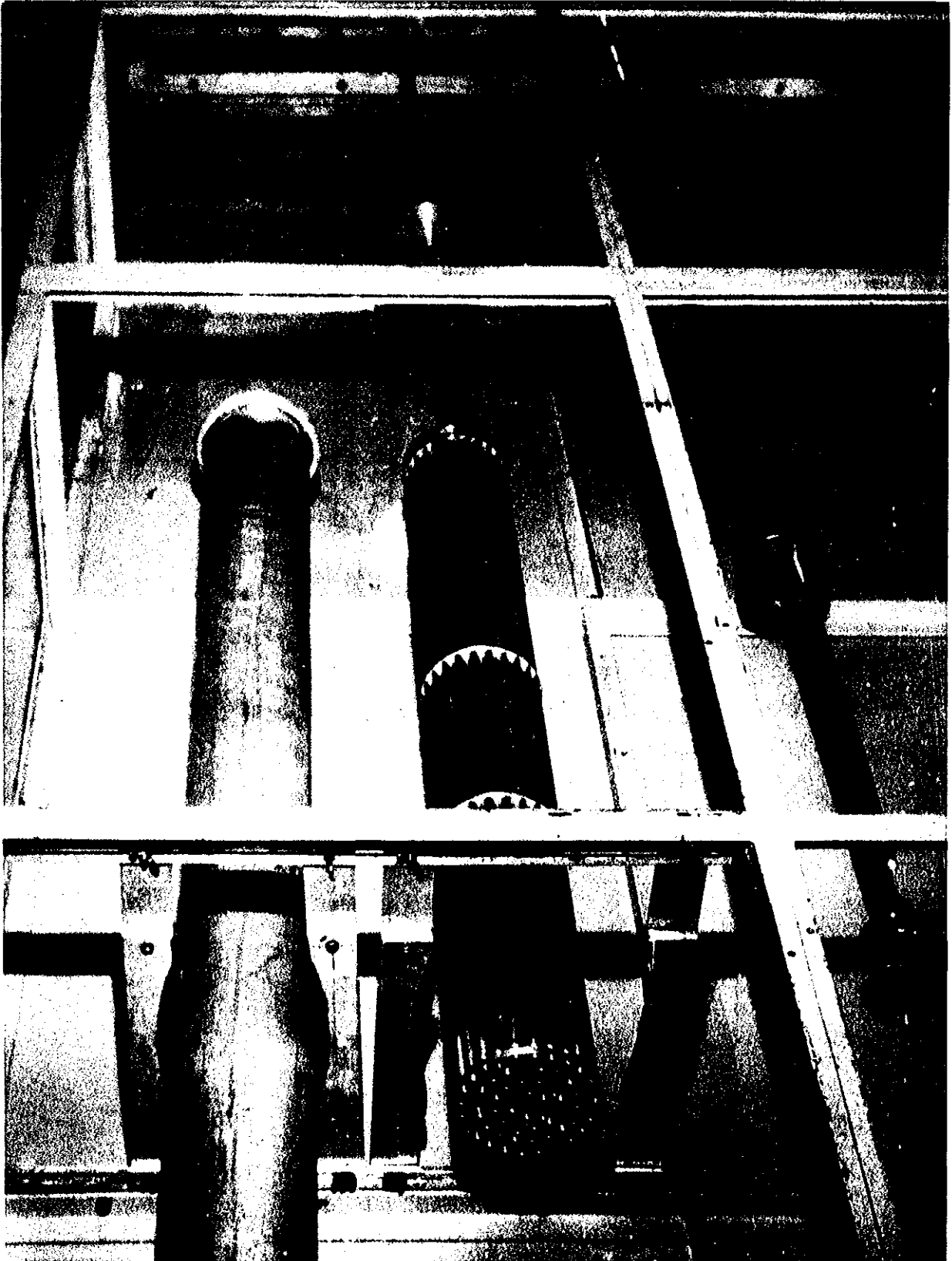
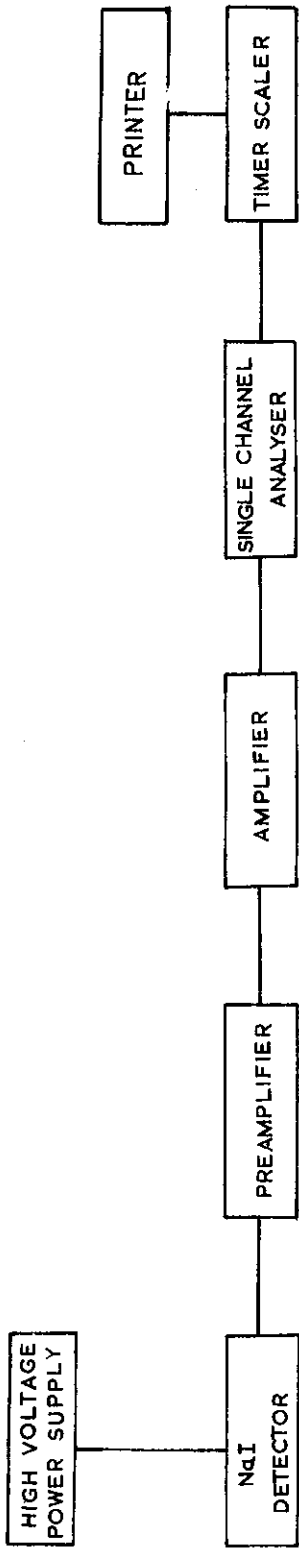
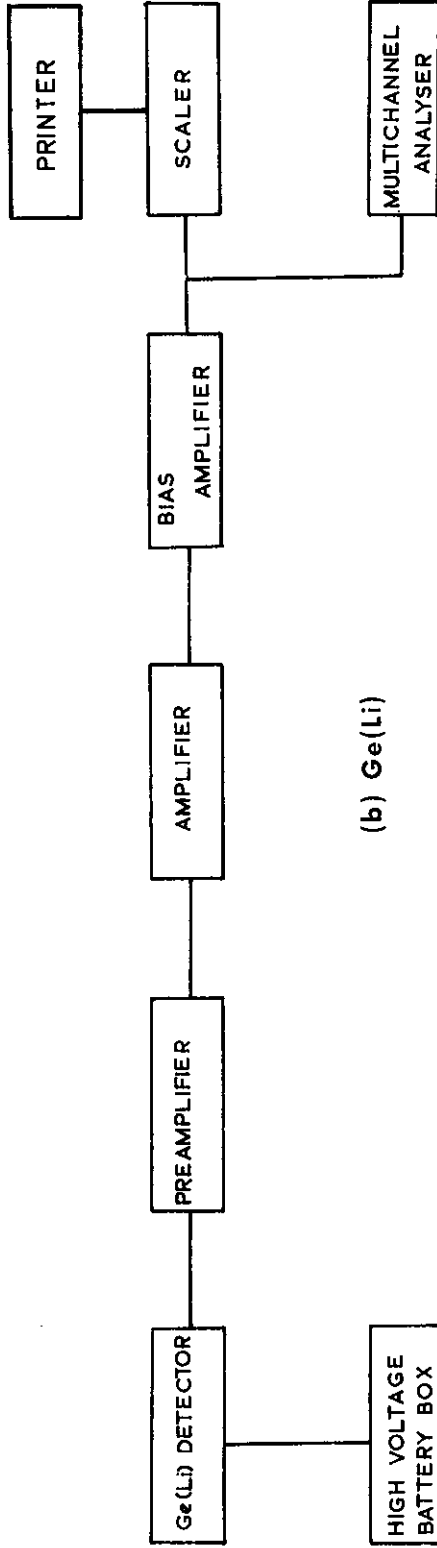


FIGURE 11. COMPLETE 37-ROD CLUSTER



(a) NaI



(b) Ge(Li)

FIGURE 12. DIAGRAMS OF ELECTRONICS USED IN COUNTING SYSTEMS

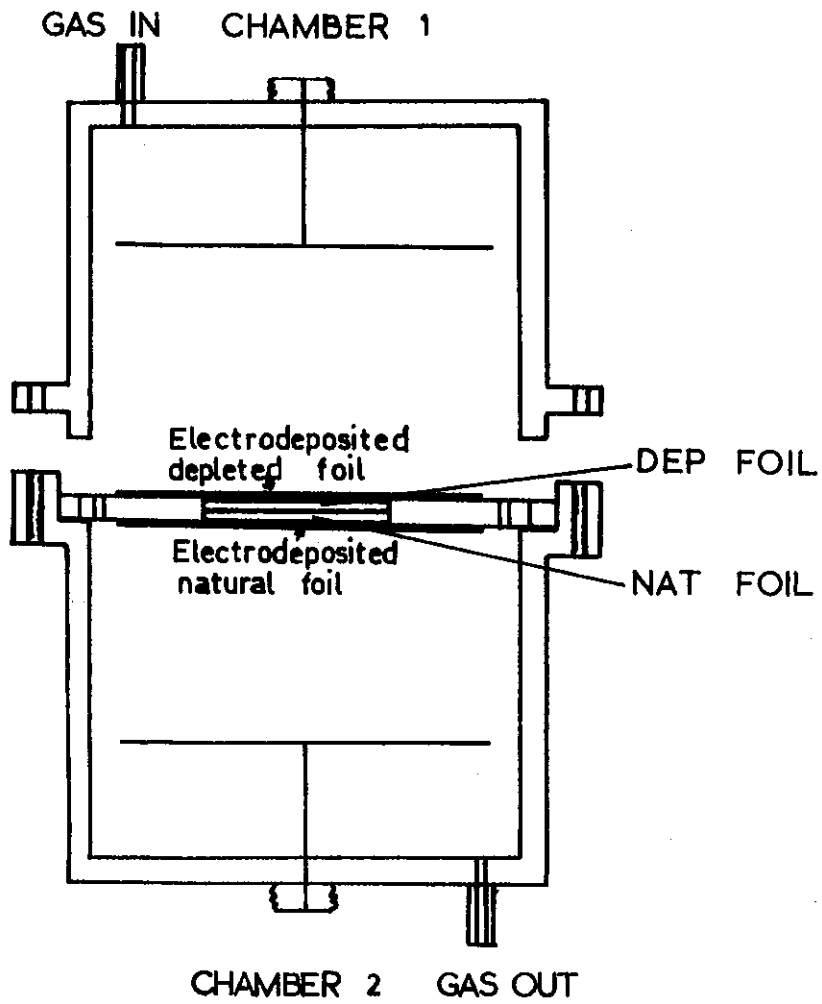


FIGURE 13. DOUBLE FISSION CHAMBER

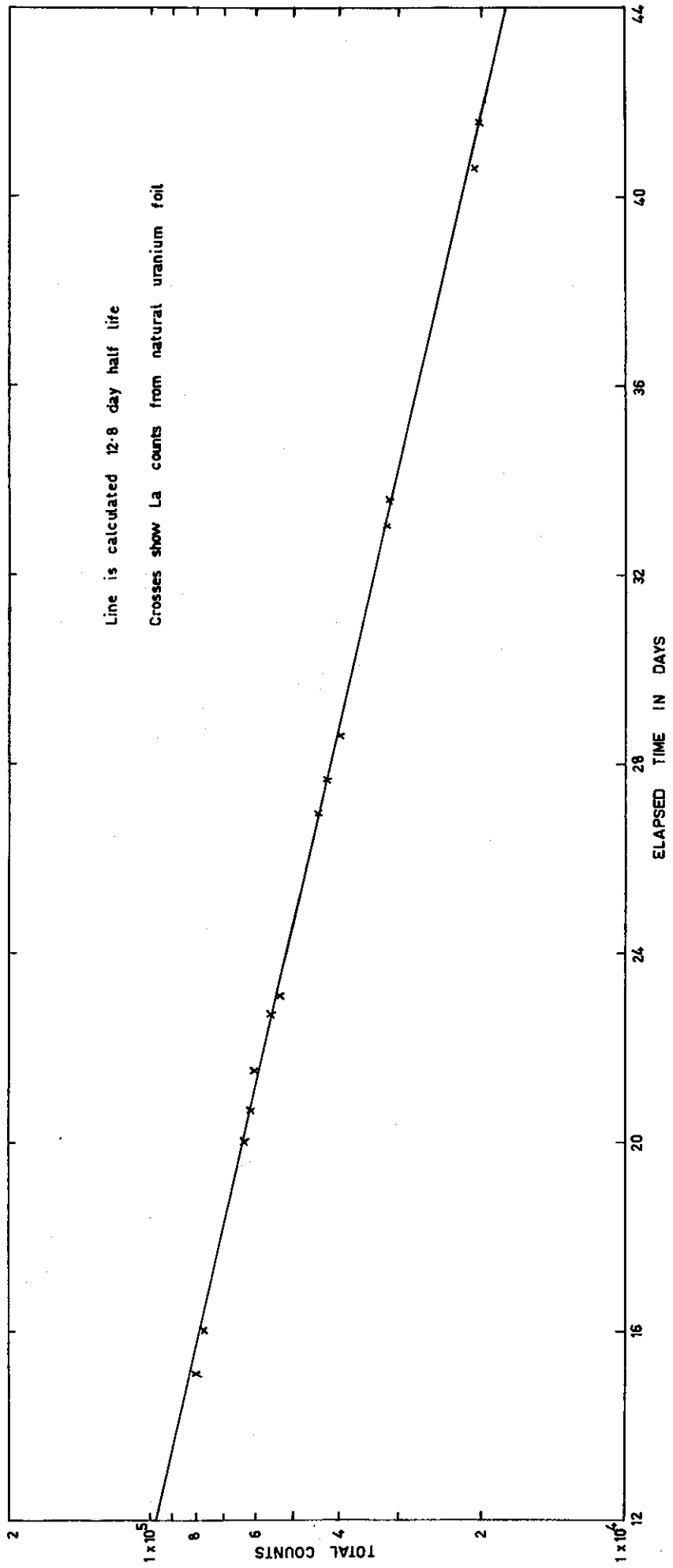


FIGURE 14. DECAY OF <sup>140</sup>La

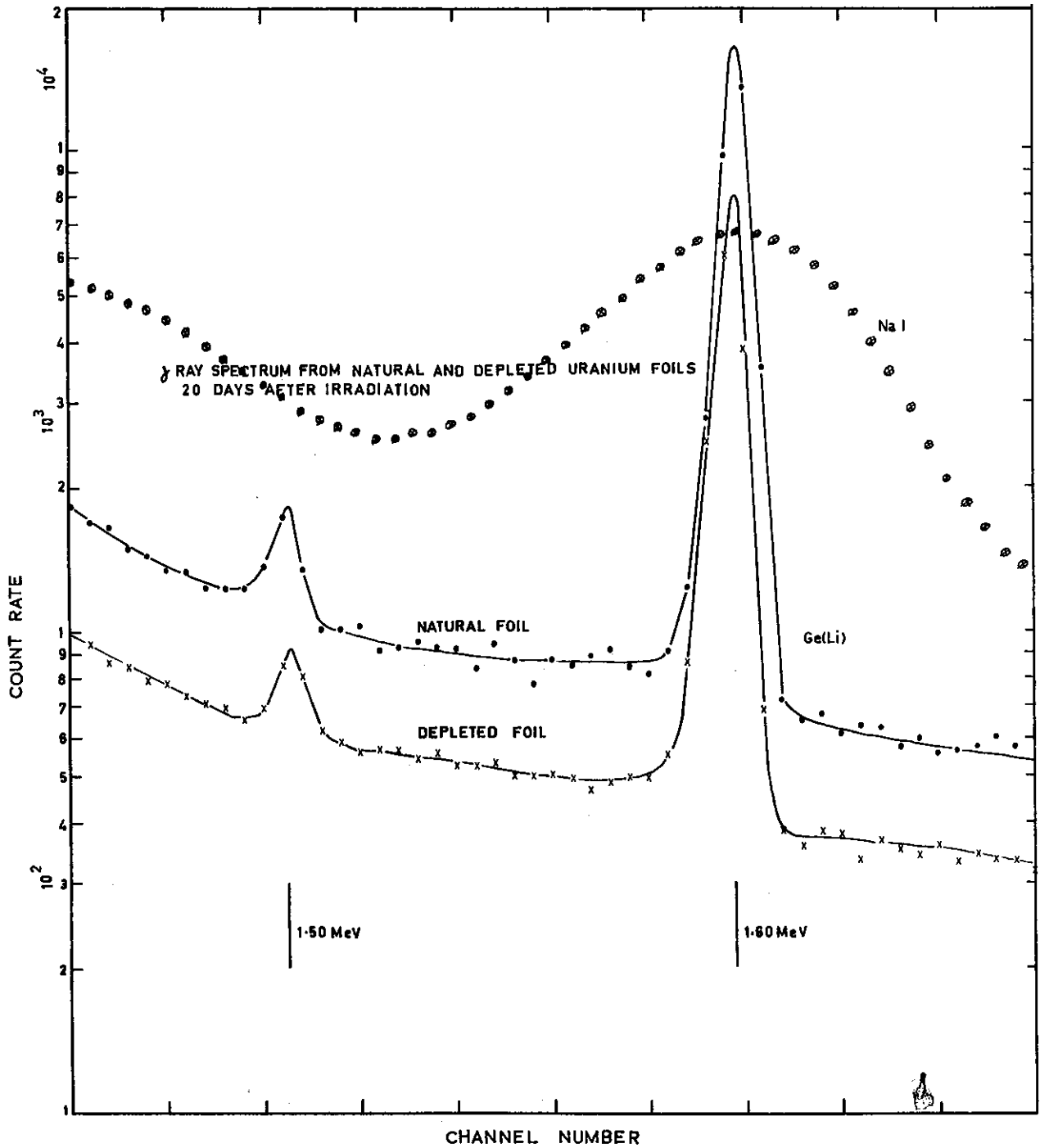


FIGURE 15. GAMMA RAY SPECTRA FROM URANIUM FISSION PRODUCTS

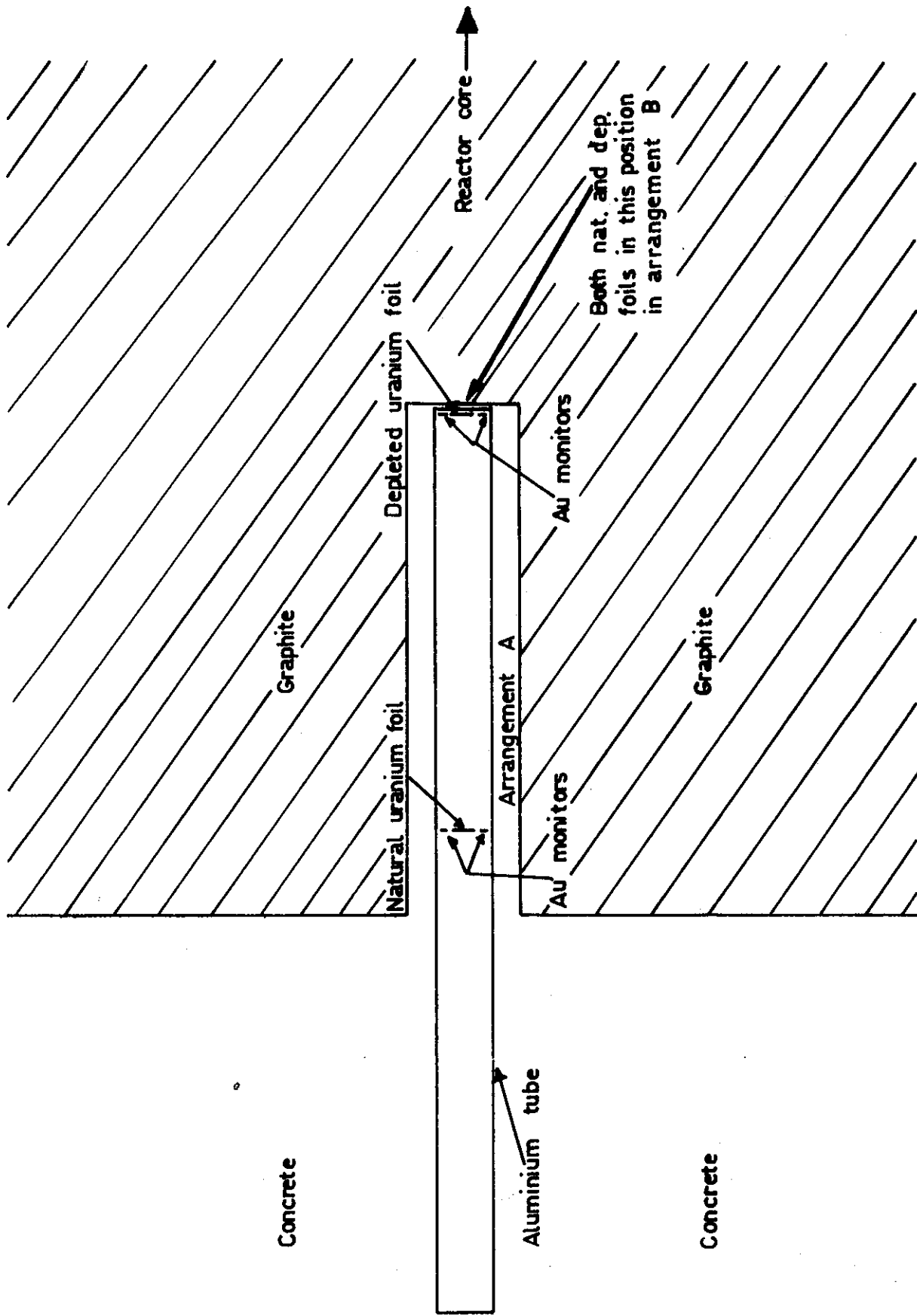


FIGURE 16. FOIL LOCATIONS IN THERMAL COLUMN

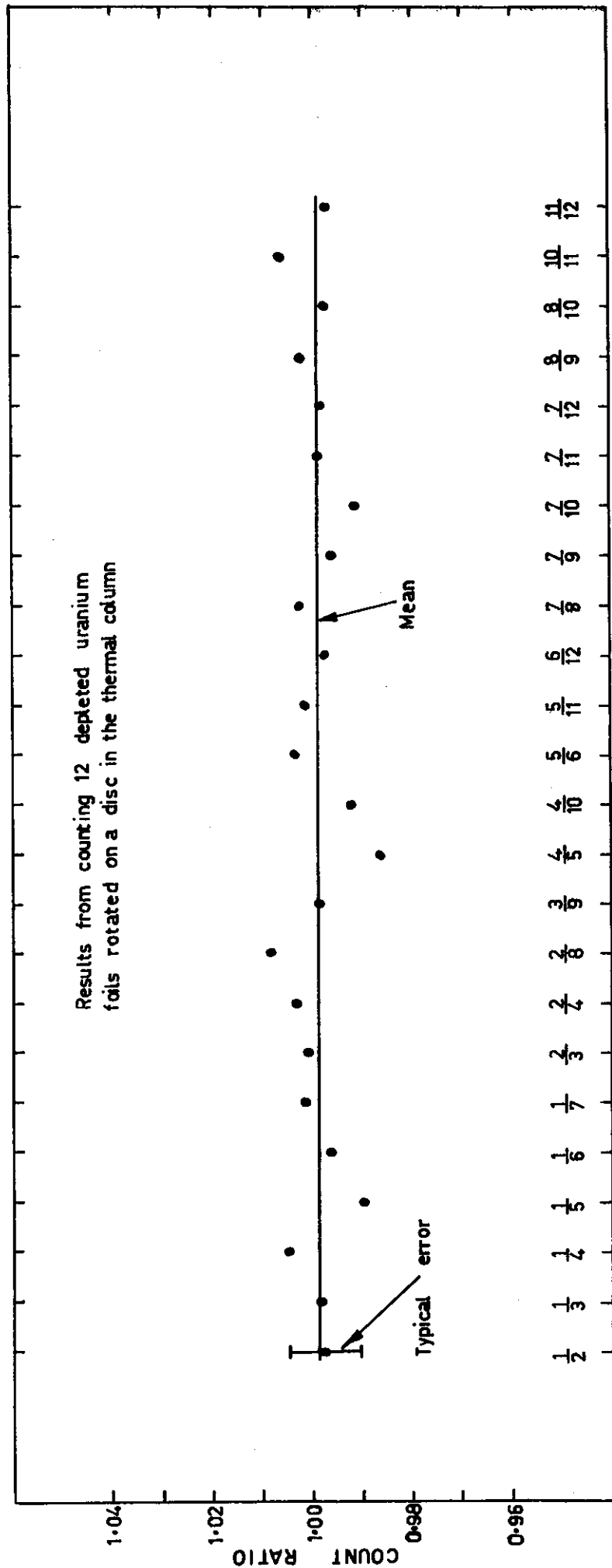


FIGURE 17. COMPARISON OF DEPLETED FOIL ENRICHMENT

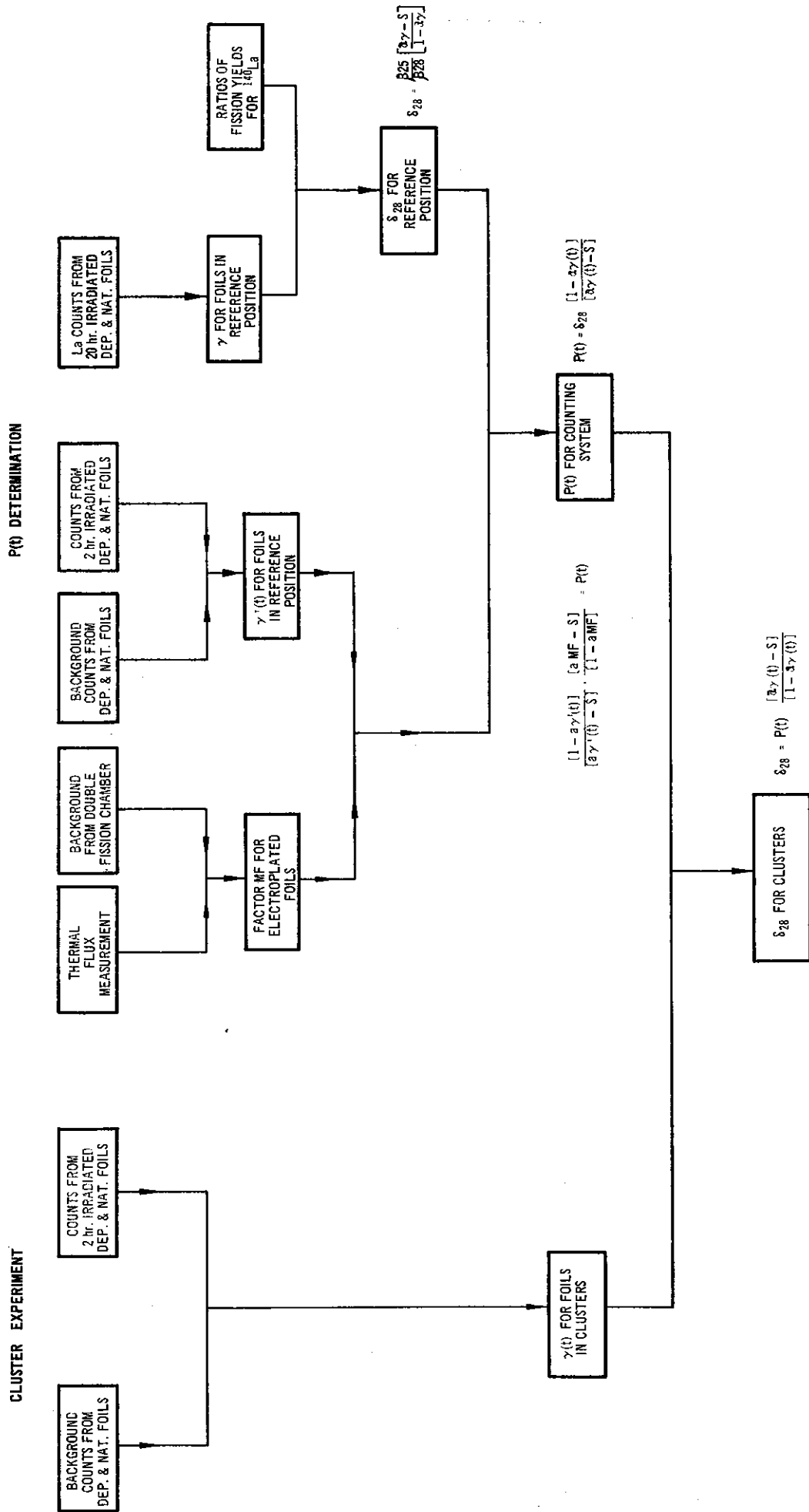
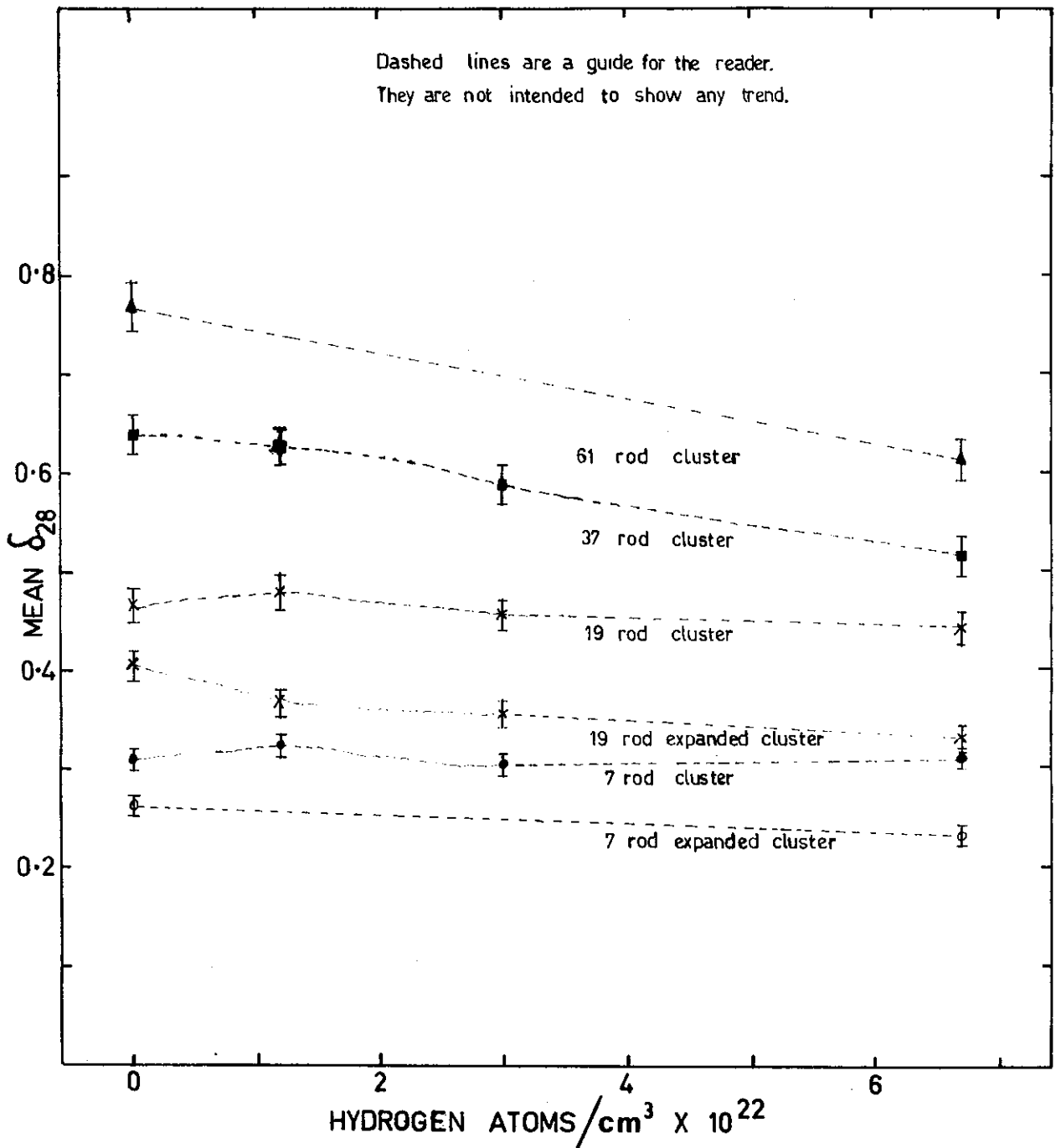


FIGURE 18. SCHEMATIC DIAGRAM SHOWING STEPS IN DETERMINATION OF  $\delta_{28}$



**FIGURE 19. VARIATION OF  $\delta_{28}$  WITH HYDROGEN ATOMS IN COOLANT FOR VARIOUS CLUSTER GEOMETRIES**

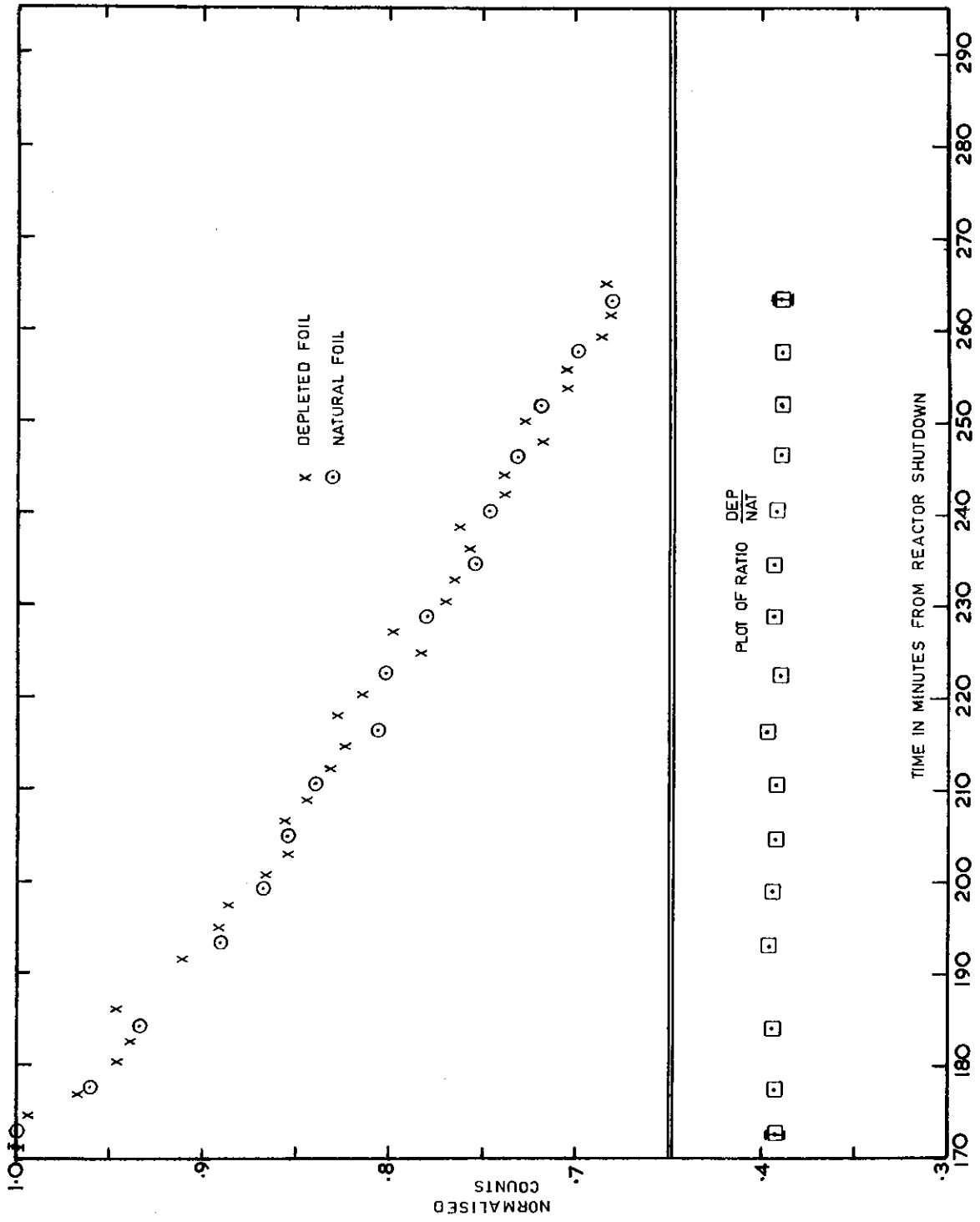


FIGURE 20. COMPARISON OF GAMMA DECAY FROM NATURAL AND DEPLETED URANIUM